NASA CONTRACTOR REPORT

NASA CR-1944

THE PRESSURE AND DEFORMATION PROFILE BETWEEN TWO COLLIDING LUBRICATED CYLINDERS

by Kwan Lee and H. S. Cheng

Prepared by
NORTHWESTERN UNIVERSITY
Evanston, Ill.
for Lewis Research Center

NATIONAL AERONAUTICS AND SPACE ADMINISTRATION • WASHINGTON, D. C. • NOVEMBER 1971

1. Report No.	2. Government Accession No.	3. Recipient's Catalog No.
NASA CR-1944		

4. Title and Subtitle
THE PRESSURE AND DEFORMATION PROFILE BETWEEN TWO COLLIDING LUBRICATED CYLINDERS

5. Report Date
November 1971

6. Performing Organization Code

7. Author(s)
Kwan Lee and H. S. Cheng

8. Performing Organization Report No.
None

10. Work Unit No.

9. Performing Organization Name and Address
Northwestern University
Evanston, Illinois

11. Contract or Grant No.
NGL-14-007-084

13. Type of Report and Period Covered
Contractor Report

12. Sponsoring Agency Name and Address
National Aeronautics and Space Administration
Washington, D.C. 20546

14. Sponsoring Agency Code

15. Supplementary Notes
Project Manager, Erwin V. Zaretsky, Fluid System Components Division, NASA Lewis Research Center, Cleveland, Ohio

16. Abstract

The pressure and deformation profiles between two colliding lubricated cylinders are obtained by solving the coupled, time-dependent elastohydrodynamic equations with an iterative procedure. The analysis includes effects which were not considered in a previous solution, namely, the effect of the lubricant compressibility and the effect of a lubricant with composite pressure-viscosity coefficients. It is found that the local approach velocity plays an important role during final stages of normal approach. It causes the lubricant to be entrapped within the contact region; neither the pressure nor the deformation profile converges to the Hertzian profile for a dry contact. The use of a smaller pressure-viscosity coefficient at high pressures reduces the sharp pressure gradient at the center of the contact and produces a much milder variation of load with respect to the film thickness. The effect of compressibility of the lubricant is found to be relatively small.

17. Key Words (Suggested by Author(s))	18. Distribution Statement
Squeeze film Elastohydrodynamics Lubrication Contacting cylinders	Unclassified - unlimited

19. Security Classif. (of this report)	20. Security Classif. (of this page)	21. No. of Pages	22. Price*
Unclassified	Unclassified	97	$3.00

* For sale by the National Technical Information Service, Springfield, Virginia 22151

TABLE OF CONTENTS

SUMMARY

Results of the present theory on the normal approach elastohydrodynamic problem show that:

1. The features of pressure and deformation profiles during the early stages of the normal approach agree well with those obtained in Ref. 4, which neglects the influence of the local approach velocity. The steepness of the pressure gradient at the center is strongly dependent upon the product of the pressure-viscosity coefficient and the center pressure. This strong dependence is removed if a smaller pressure-viscosity coefficient is used at high pressures.
2. During final stages of the normal approach, present theory yields considerably different results from those in Ref. 4. The local approach velocity at the edge of the contact region becomes far greater than the center approach velocity, and finally entraps a pocket of the lubricant at the center of the contact. Both the deformation and pressure profiles never converge to the dry contact Hertzian distribution.
3. For a normal approach process under a constant load, the maximum center pressure can exceed that of the maximum Hertzian pressure depending upon the pressure-viscosity coefficient. By introducing the composite-exponential model for the pressure-viscosity dependence, the maximum center pressure is much reduced.
4. The inclusion of the lubricant compressibility in the analysis gives arise to a slightly higher load than the incompressible solution.

CHAPTER 1 - INTRODUCTION

1.1 Introduction

Whenever any two lubricated contacts approach each other along their common normal under a heavy load, highly localized pressures are generated by the squeeze film action within the conjunction. The determination of the pressure distribution due to the squeeze action considering the surface deformation is known as the normal approach problem in elastohydrodynamic (EHD) lubrication.

The squeeze-film action occurs frequently in many machine components such as gear teeth contacts, cams, and rolling element bearings during transient loadings. The normal approach problem has a special significance in the so-called partial EHD contacts in which the asperity heights approach the same order of magnitude as the film thickness. Under these conditions, the entering of any asperity into the conjunction zone is equivalent to the squeeze-film EHD problem between a contacting body and a flat plate.

Mathematically, the normal approach problem differs considerably from the conventional rolling and sliding EHD theories [1,2,3]. For the rolling problem, the pressure and film distributions are steady-state: whereas for squeeze-film problem they are time-dependent and must be obtained by solving the transient Reynolds equation coupled with the elasticity equation. Because the pressure gradient varies inversely with the third power of the film thickness and the viscosity for most lubricants varies exponentially with pressure, the two coupled equations are highly nonlinear. So far, no analytical solution has been found for these equations.

In 1961, Christensen [4] introduced the first numerical solution to the present EHD problem for an incompressible lubricant with an exponentially varying viscosity. In his solution, he has neglected the squeeze-film action due to the change of deformation. This effect was recently shown to be significant at small film thickness by Herrebrugh [5] in a semi-analytical solution for an isoviscous and incompressible lubricant. Moreover, Christensen was not able to obtain convergent solutions in the final stage of the normal approach because of numerical difficulties.

The present investigation is aimed toward seeking a more effective numerical solution for the transient EHD problem which is capable of achieving the following:

1. remove the convergence difficulties at small film thickness,
2. incorporate the effect of deformation rate,
3. admit any arbitrary variation of viscosity with pressure,
4. incorporate the effect of the lubricant compressibility.

1.2 Previous Investigations

In spite of the practical significance of the normal approach problem, it has received relatively little attention in the literature. Before the theories of EHD had been fully developed, Bowden and Tabor [6] studied the nature of contact between two colliding solids - the collision between a soft metal surface and a steel ball when it is dropped from a certain height. Initially, they were concerned with the plastic deformation on the dry metal surface by the hard ball dropped from a measured height. The initial contact is so small

that the impact pressure momentarily reached a value higher than the yield stress of the soft metal. The permanent indentation occurred on the flat surface when a ball of 1 cm diameter was dropped from a height of only 2 cm. To examine the effect of lubricant on the indentation, they lubricated the flat surface with a viscous fluid, and by the electrical conductance method, they detected metallic contact and the duration of contact before the ball rebounded. The experiment with a less viscous lubricant did not give any different results compared with those of the dry contact case. The amount of metallic contact and the impact time were not altered. However, the experiment with a highly viscous fluid showed that during impact metallic contact did not occur at all, but the flat surface yielded leaving a permanent indentation. This means that the fluid pressure in the contact zone at any stage increased beyond the yield stress of the soft metal. They explained the phenomenon of surface separation by comparing the impact time with the time required to have the fluid in the contact region squeezed out completely. If the impact time is less than the squeezing time which depends upon fluid viscosity, then direct metallic contact is not possible. It is also seen from their experiment that the permanent indentation on the lubricated flat surface showed a sharp conical shape with the central depth deeper than that of the spherical indentation produced by dropping the ball on a flat surface from the same height.

For the first time, Christensen [4] made a theoretical study of the normal approach problem of two cylinders in which he considered the viscosity of fluid varies exponentially with pressure and the

contact surfaces are elastic. He solved simultaneously the two governing equations - the transient Reynolds equation and the elasticity equation - in time sequence as the gap between the two cylinders decreases. By assuming that the velocity normal to the contacting surface is uniform within the film, and by employing a direct - iterative procedure, he was able to obtain a converging solution for successive intervals during the normal approach. However, when the gap becomes very thin, the numerical procedure using the direct iteration method presents great difficulties and Christensen was not able to obtain the convergent solutions in this important region. Moreover, the assumption of a uniform velocity is valid only when the film thickness is large compared to the deformation. For the small film thichnesses, the local normal velocity not only exceeds the center normal velocity but also varies drastically along the contact surface. As it will be seen later in this work, the local normal velocity at the minimum gap can be order of magnitude more than the center velocity.

Based on his theoretical work, Christensen concluded:

1. When two elastic cylinders, lubricated with oils whose viscosity varies exponentially with pressure, approach each other, very high pressures in excess of the maximum Hertzian pressure can be developed in the fluid film. The elastic deformation forms a pocket shape with the

contact. As the film thickness further reduces, the deformation tends to flatten out and eventually converges to the shape of a Hertzian flat.

2. For a given load applied to the cylinders, the maximum pressure at the contact center depends upon the parameter, αE. Harder material and oil with a high α yield a higher center pressure during the approach.

To make qualitative comparisons with his theoretical results, Christensen also conducted a series of experiments similar to Bowden and Tabor's work [6] by dropping a ball on a lubricated flat surface from a predetermined height. The main objective in his experiment was to determine the effects of material properties on the permanent indentation on the flat surface. To achieve this, he used several pairs of balls and flat surfaces having different material properties.

He succeeded in proving that under a constant load, the maximum transient pressure in the fluid film increases when the parameter αE increases. However, he emphasized that this correlation is strictly qualitative since the theory is based on the assumptions of an elastic cylinder, whereas the actual experiment involves elastic-plastic deformations between a sphere and a flat.

Recently, Herrebrugh [5], in an attempt of solving the normal approach problem of two cylinders, formulated a single governing equation by combining the Reynolds equation and the elasticity equation. Since he obtained the solution only for the isoviscous case which is far removed from the reality of the problem, his solution is not complete and his method of solution eventually relies on the

numerical method, it is hard to see any advantage in his solution scheme. The solution of this integral-differential equation - the governing equation - is obtained by the method of successive approximations with a semi-numerical procedure. He obtained solutions for the isoviscous case with the same assumption used by Christensen, that is, the normal velocity is uniform within the contact. However, his solution only covers regions of high and moderate film thicknesses. For extremely thin films, the method of successive approximations fails to converge.

Herrebrugh also noted that as the film becomes small, the ratio of the local velocity to the center velocity begins to depart from unity. This demonstrates that the assumption of a uniform velocity is no longer valid at small film thicknesses. For the isoviscous case at the small film thickness where he begins to experience convergence difficulty, the ratio of local velocity to center velocity varies from 0.75 to 1.25. It will be shown in the present work that the pressure-viscosity relation has a very strong influence on the ratio of local to center velocity at small film thickness. When the effect of variable viscosity is included in the solution, the local velocity at the edge of the contact can be as many as ten times the center velocity.

CHAPTER 2 - MATHEMATICAL FORMULATION

2.1 Geometry

As shown on Fig. 1-1(a), when the two cylinders approach each other along the line connecting their geometrical centers under a heavy load, the lubricant between them is pressurized by the squeezing action of the two cylinders. The contact region where the pressure is much higher than the ambient pressure is very narrow compared with the radius of the cylinder. This fact will be utilized in the development of the film thickness formula. The present analysis is mainly concerned with the phenomena occurring in this narrow contact region during the normal approach of the two cylinders.

In order to facilitate the mathematical analysis of the problem, the contact between the two cylinders as shown on Fig. 1-1(a) is replaced by the equivalent cylinder with a near-by plane as shown on Fig. 1-1(b). The geometrical requirement for this conversion is that at equal value of x the separation between the two cylinders should be the same as that between the equivalent cylinder and the flat surface.

From Fig. 1-1(a),

$$h_g = h_o' + R_1\left[1 - \left(1 - \left(\frac{x}{R_1}\right)^2\right)^{1/2}\right] + R_2\left[1 - \left(1 - \left(\frac{x}{R_2}\right)^2\right)^{1/2}\right] \qquad (1)$$

where h_g is called the geometrical film thickness and h_o' is the separation on the line of centers.

Eq. (1) can be expanded to give,

$$h_g = h'_o + R_1 \left(\frac{1}{2}\left(\frac{x}{R_1}\right)^2 + \frac{1}{8}\left(\frac{x}{R_1}\right)^4 -- \right) + R_2 \left(\frac{1}{2}\left(\frac{x}{R_2}\right)^2 + \frac{1}{8}\left(\frac{x}{R_2}\right)^4 + -- \right) \qquad (2)$$

Since the width of the contact region is very small, $(\frac{x}{R_1})$ and $(\frac{x}{R_2})$ are both small compared to unity. Thus, by neglecting the terms higher than the second power in Eq. (2), we obtain the approximate separation between the two cylinders,

$$h_g \cong h'_o + \frac{x^2}{2}\left(\frac{1}{R_1} + \frac{1}{R_2}\right) \qquad (3)$$

Eq. (3) can be rewritten as,

$$h_g \cong h'_o + \frac{x^2}{2R} \qquad (4)$$

where $\frac{1}{R} = \frac{1}{R_1} + \frac{1}{R_2}$.

If the radius of the equivalent cylinder is

$$R = \frac{R_1 R_2}{R_1 + R_2} \quad , \qquad (5)$$

then the geometrical requirement for the conversion from Fig. 1-1(a) to Fig. 1-1(b) is satisfied.

2.2 Governing Equations

2.2.1 Elasticity Equation

In the development of the displacement equation a number of

assumptions can be made based on the relatively small width of the contact region where the pressure is higher than the atmospheric pressure: the contact region is very small compared with the radius and the length of the cylinder; the displacement is in the state of plane strain; and the tangential displacement is neglected because it does not have significant effects on the lubricated contact surface. The normal displacement by the pressure in the fluid film is calculated on the semi-infinite plane and then added to the rigid geometrical film thickness. The displacement equation is derived in Appendix A and is shown below,

$$d(x,t) = -\frac{2(1-\nu^2)}{\pi E}\int_{-\infty}^{\infty} P(\xi,t)\ln|\xi - x|\, d\xi + C \qquad (6)$$

The constant C is eliminated by including it in the center film thickness formula. Due to this constant the displacement is not absolute but a relative quantity.

The film thickness between two cylinders is the sum of the rigid geometrical film thickness and the deformations - displacements - of two cylinders.

$$h(x,t) = h_o'(t) + \frac{x^2}{2R_1} + \frac{x^2}{2R_2} + d_1(x,t) + d_2(x,t) + c_1 + c_2 \qquad (7)$$

From Eq. (7),

$$h(o,t) = h_o'(t) - \frac{2(1 - \nu_1^2)}{\pi E_1} \int_{-\infty}^{\infty} p(\xi,t) \ln|\xi| d\xi$$

$$- \frac{2(1 - \nu_2^2)}{\pi E_2} \int_{-\infty}^{\infty} p(\xi,t) \ln|\xi| d\xi + c_1 + c_2 \tag{8}$$

From Eq. (8),

$$c_1 + c_2 = h(o,t) - h_o'(t) + \frac{2(1 - \nu_1^2)}{\pi E_1} \int_{-\infty}^{\infty} p(\xi,t) \ln|\xi| d\xi$$

$$+ \frac{2(1 - \nu_2^2)}{\pi E_2} \int_{-\infty}^{\infty} p(\xi,t) \ln|\xi| d\xi \tag{9}$$

Substituting Eq. (9) for $c_1 + c_2$ in Eq. (7) we obtain

$$h(x,t) = h(0,t) + \frac{x^2}{2R_1} + \frac{x^2}{2R_2} - \frac{2(1 - \nu_1^2)}{\pi E_1} \int_{-\infty}^{\infty} p(\xi,t) \ln \frac{|\xi - x|}{|\xi|} d\xi$$

$$- \frac{2(1 - \nu_2^2)}{\pi E_2} \int_{-\infty}^{\infty} p(\xi,t) \ln \frac{|\xi - x|}{|\xi|} d\xi \tag{10}$$

Let $h(o,t) = h_o(t)$, which is the center film thickness including implicitly the center deformation.

Define E as,

$$\frac{1}{E} = \frac{1}{2} \left(\frac{1 - \nu_1^2}{E_1} + \frac{1 - \nu_2^2}{E_2} \right) \tag{11}$$

where E_1, E_2 and ν_1, ν_2 are Young's modulus and Poisson's

ratio of cylinders 1 and 2, respectively.

Using Eq. (11) for E and recalling $\frac{1}{R} = \frac{1}{R_1} + \frac{1}{R_2}$, Eq. (10) becomes,

$$h(x,t) = h_o(t) + \frac{x^2}{2R} - \frac{4}{\pi E} \int_{-\infty}^{\infty} p(\xi,t) \ell n \frac{|\xi - x|}{|\xi|} d\xi \qquad (12)$$

which is the film thickness between the equivalent cylinder and the flat surface.

2.2.2 Hydrodynamic Equation

The inertia force in the flow field between two cylinders is negligible compared to the viscous force, which is the fundamental assumption in the derivation of Reynolds equation. In the present study the transient, one dimensional Reynolds equation is taken as a governing equation for pressure distribution. The one dimensional equation is justified by the fact that the length of the cylinder can be assumed to be infinite if it is compared with the width of the contact region. Further assumptions made in the hydrodynamic equation are: 1) the flow is isothermal and 2) the weight of the cylinder is negligible in comparison with the external force.

The governing equation for pressure distribution is

$$\frac{\partial}{\partial x}\left(\frac{\rho h^3}{12\mu} \frac{\partial p}{\partial x}\right) = \frac{\partial(\rho h)}{\partial t} \qquad (13)$$

Due to the symmetry of the contact surface at x = 0, the profiles of pressure and film thickness are symmetrical at x = 0.

The boundary conditions for Eq. (13) are

$$p = 0 \qquad \text{at } x = -\infty$$

$$\frac{\partial p}{\partial x} = 0 \qquad \text{at } x = 0 \tag{14}$$

Eq. (13) is integrated from x = - x to x = 0 using the second boundary condition of (14), thus we obtain

$$\frac{\partial p}{\partial x} = -\frac{12\mu}{\rho h^3} \int_{-x}^{o} \frac{\partial(\rho h)}{\partial t}\, dx \tag{15}$$

A new variable Q is introduced in order to facilitate the use of several viscosity function in the governing equation. Q is defined as:

$$Q = 1 - \frac{1}{\bar{\mu}} \tag{16}$$

where $\bar{\mu} = \frac{\mu}{\mu_s}$ and μ_s is the ambient viscosity.

The spatial derivative of Q is

$$\frac{\partial Q}{\partial x} = \frac{1}{\bar{\mu}} \frac{\partial(\ell n\ \bar{\mu})}{\partial p} \frac{\partial p}{\partial x} \tag{17}$$

The pressure derivative in Eq. (15) is replaced by Eq. (17), thus we obtain

$$\frac{\partial Q}{\partial x} = - \frac{12\ \mu_s}{\rho h^3} \frac{\partial(\ell n\ \bar{\mu})}{\partial p} \int_{-x}^{\infty} \frac{\partial(\rho h)}{\partial t}\, dx \qquad (18)$$

In the above equation the viscosity term is replaced by $\frac{\partial(\ell n\ \bar{\mu})}{\partial p}$ which is the simple pressure - viscosity coefficient if $\bar{\mu}$ is an exponential function of p.

Integrating Eq. (18) from $x = -\infty$ to x gives

$$Q - Q_{-\infty} = - 12\ \mu_s \int_{-\infty}^{x} \left[\frac{1}{\rho h^3} \frac{\partial(\ell n\ \bar{\mu})}{\partial p} \int_{-x}^{\infty} \frac{\partial(\rho h)}{\partial t}\, d\xi\right] dx \qquad (19)$$

where $Q_{-\infty} = 0$ because at $x = -\infty$ the viscosity is the same as the ambient viscosity.

The value of Q at the film center is

$$Q_o = - 12\ \mu_s \int_{-\infty}^{\infty} \left[\frac{1}{\rho h^3} \frac{\partial(\ell n\ \bar{\mu})}{\partial p} \int_{-x}^{\infty} \frac{\partial(\rho h)}{\partial t}\, d\xi\right] dx \qquad (20)$$

The above equation will be used in the calculation of the center approach velocity.

The instantaneous load per unit width of the cylinder is the integral of the pressure distribution

$$w(t) = \int_{-\infty}^{\infty} p(x,t)dx \qquad (21)$$

2.2.3 Approaching Velocity

Since the deformation term in Eq. (12) is the relative defor-

mation based on the center deformation which is not known, the approach velocity is also the relative velocity, not the absolute velocity. However, the relative approaching velocity is incorpoated in the formation of the present problem because, in general, the difference between these two velocities is extremely small in the regime of elastohydrodynamic lubrication. Of course, if one would attempt to solve the impact problem of two cylinders like the experiment of [6], he should find the absolute velocity which plays the important role in the solution of the impact problem.

Differentiating Eq. (12) with respect to time we obtain

$$\frac{\partial h(x,t)}{\partial t} = \frac{\partial h_o(t)}{\partial t} - \frac{4}{\pi E} \frac{\partial}{\partial t} \int_{-\infty}^{\infty} p(\xi,t) \ell n \frac{|\xi - x|}{|\xi|} d\xi \qquad (22)$$

It is thus seen that the local approaching velocity consists of two terms: the first is the approach velocity of the contact center and the second is the velocity due to deformation-deformation velocity - which is also dependent on time and varies along the contact surface.

Let $v_o = - \frac{\partial h_o}{\partial t}$ and $v_d = \frac{4}{\pi E} \frac{\partial}{\partial t} \int_{-\infty}^{\infty} p(\xi,t) \ell n \frac{|\xi - x|}{|\xi|} d\xi$

then Eq. (22) can be written as:

$$\frac{\partial h}{\partial t} = - v_o - v_d \qquad (23)$$

2.3 Viscosity and Density Variations

Both the viscosity and the density of the lubricant are assumed to be functions of pressure only. Two types of viscosity functions have been used in the present analysis. The first type is the straight exponential relation between the viscosity and pressure. This relation can be expressed as

$$\mu = \mu_s e^{\alpha p} \tag{24}$$

The second type is the so-called composite-exponential relation between the viscosity and pressure. In this relation, the viscosity increases exponentially with pressure according to a large exponent in the low pressure region and much smaller exponent in the high pressure region. Mathematically, it can be expressed as

$$\mu = \mu_s e^{\alpha p} \qquad \text{for } p \leq p_1$$

$$\mu = \mu_s e^{(\alpha p_1 + \beta(p - p_1))} \qquad \text{for } p > p_2 \tag{25}$$

where p_1 = 40,000 psi and p_2 = 70,000 psi.

The viscosity between p_1 and p_2 is increased asymptotically as shown on Fig. 1-2.

The composite model was first introduced by Allen, Townsend and Zaretsky [7]. Their viscosity vs. pressure curve consists of two straight lines on the semi-log paper with a discontinuous viscosity gradient at p = 55,000 psi. Since this discontinuous gradient is

physically inconceivable, before employing their viscosity function in the present analysis the discontinuity is removed as mentioned in the above paragraph. Their theoretical spinning torque based on this empirical equation of viscosity matched excellently with their measured torque. The moderation of viscosity increase at high pressure seems to be quite reasonable though the exact behavior of the lubricant under the dynamic conditions is not known.

The primary purpose of employing the composite-exponential lubricant in the present analysis is to understand what effects this lubricant may exhibit on the pressure, film thickness, load and approach velocity. By comparing the two solutions - the one based on the straight exponential lubricant and the other on the composite - exponential lubricant - one would come up with the plausible conclusion on which lubricant model yields the realistic solution in respect to pressure and load during the normal approach.

To find out the effect of α alone on the pressure profile, the two different values of α in the straight exponential lubricant are used in this investigation.

The density function used in this investigation is

$$\rho = \rho_s\left(1 + \frac{bp}{1 + a_1 p}\right) \tag{26}$$

where ρ_s is the ambient density, and a_1 and b are the coefficients determined from ASME Report [8]. Eq. (26) was originally introduced by Dowson and Whitaker [9].

2.4 Formulation of Elastohydrodynamic Problem

2.4.1 Coupled Time-Dependent Elastohydrodynamic Equations

It has been shown in many previous works on EHD lubrications that the solutions for pressure and film thickness must be compatible with each other, i.e., the pressure profile obtained from the hydrodynamic equation with a certain film thickness profile must be equal to the pressure profile required to deform the contact surface to the same film thickness. This demands that the hydrodynamic equation and the elasticity equation be solved simultaneously at each instantaneous location of the cylinder.

The two major equations to be solved simultaneously for the pressure and film thickness are:

$$\frac{\partial p}{\partial x} = - \frac{12\mu}{\rho h^3} \int_{-x}^{o} \frac{\partial(\rho h)}{\partial t} \, dx \tag{15}$$

$$h = h_o + \frac{x^2}{2R} - \frac{4}{\pi E} \int_{-\infty}^{\infty} p(\xi,t) \ell n \frac{|\xi - x|}{|\xi|} \, d\xi \tag{12}$$

2.4.2 Normalization

Introduce the following non-dimensional variables,

$$P = \frac{p}{p_o} \quad , \quad H = \frac{h}{R} \quad , \quad H_o = \frac{h_o}{R} \quad , \quad X = \frac{x}{a} \quad ,$$

$$Z = \frac{\xi}{a} \quad , \quad V_o = \frac{12\mu_s}{ER} v_o, \quad V = \frac{12\mu_s}{ER} v \quad , \quad D = \frac{d}{R} \quad , \tag{27}$$

$$T = \frac{v_o}{R} t, \quad P_{HZ} = \frac{p_o}{E} \quad , \quad \frac{a}{R} = 4P_{HZ} \quad , \quad \bar{\beta} = \frac{\beta}{p_o} \quad ,$$

$$W = \frac{w}{ER_p} \quad , \quad \bar{\rho} = \frac{\rho}{\rho_s} \quad , \quad \bar{\alpha} = \frac{\alpha}{p_o} \quad , \quad A_1 = \frac{a_1}{p_o} \qquad (27) \text{ cont.}$$

where a is the Hertzian half-width and the subscript "o" indicates the variables at the film center.

The normalized governing equations are written as:

$$\frac{\partial P}{\partial X} = - \left(\frac{16P_{HZ}V_o\bar{\mu}}{H^3\bar{\rho}}\right) \int_{-X}^{o} \frac{\partial(\bar{\rho}H)}{\partial T} \, dX \qquad (28)$$

$$H = H_o + 8P_{HZ}{}^2X^2 - \left(\frac{16P_{HZ}{}^2}{\pi}\right) \int_{-\infty}^{\infty} P(Z,T) \ell n \frac{|Z - X|}{|Z|} \, dZ \qquad (29)$$

Eq. (19) and (20) are normalized as follows:

$$Q = - \left(16P_{HZ}V_o\right) \int_{-\infty}^{-X} \left[\frac{1}{\bar{\rho}H^3} \frac{\partial(\ell n \, \bar{\mu})}{\partial P} \int_{-X}^{o} \frac{\partial(\bar{\rho}H)}{\partial T} \, dZ\right] dX \qquad (30)$$

$$Q_o = - \left(16P_{HZ}V_o\right) \int_{-\infty}^{o} \left[\frac{1}{\bar{\rho}H^3} \frac{\partial(\ell n \, \bar{\mu})}{\partial P} \int_{-X}^{o} \frac{\partial(\bar{\rho}H)}{\partial T} \, dZ\right] dX \qquad (31)$$

The dimensionless load becomes

$$W = \frac{1}{4P_{HZ}{}^2} \int_{-\infty}^{\infty} P(X,T) dX \qquad (32)$$

The dimensionless normal velocity is obtained by differentia-

ting Eq. (29),

$$\frac{\partial H}{\partial T} = -1 - \left(\frac{16P_{HZ}^2}{\pi}\right) \frac{\partial}{\partial T} \int_{-\infty}^{\infty} P(Z,T) \ln \frac{|Z - X|}{|Z|} dZ \qquad (33)$$

$$V = -V_o \left[1 + \left(\frac{16P_{HZ}^2}{\pi}\right) \frac{\partial}{\partial T} \int_{-\infty}^{\infty} P(Z,T) \ln \frac{|Z - X|}{|Z|} dZ\right] \qquad (34)$$

From Eq. (31), we obtain the center normal velocity V_o

$$V_o = \frac{-Q_o}{16P_{HZ} \int_{-\infty}^{o} \left[\frac{1}{\bar{\rho}H^3} \frac{\partial(\ln \bar{\mu})}{\partial P} \int_{-X}^{o} \frac{\partial(\bar{\rho}H)}{\partial T} dZ\right] dX} \qquad (35)$$

2.5 Method of Solution

2.5.1 Outline of Approach

Since the pressure and film profiles are symmetrical with respect to the center of the contact, it is necessary only to obtain solutions for half of a contact. For the present analysis, the solutions are obtained in the left half of the contact. This half region is further divided into two regions - the inlet and the middle region. The division is made in such a way that in the middle region the pressure gradient is far steeper than the mild pressure increase in the inlet region.

In the inlet region, the pressure variation is less abrupt, and the method of direct iteration can be applied here without introducing any convergence difficulties. In the direct itera-

tion, the pressure is calculated by the direct integration of the hydrodynamic equation for the previously iterated film profile, and the succeeding film profile is calculated by integrating the elasticity equation according to the newly integrated pressure profile. This method is simple and efficient, but is only effective for cases of relatively large film thickness. As demonstrated by Christensen [4], for extremely small film thickness, the direct iteration fails to yield a convergent solution.

In the middle region, the system uations are solved by Newton-Raphson method. The solution of the system equations gives the pressure correction at every grid point. The Newton-Raphson method is very effective in solving a system of nonlinear equations and usually yields the converged solution in several iterations. One drawback in the Newton-Raphson method is the calculation of partial derivatives of all the variables in the system equations and the inversion of the matrix of which elements consist of these derivatives. A substantial portion of the calculating time for the present problem is expended in the operation of the matrix inversion. Details of numerical treatment for the inlet as well as for the middle region are given in the next sections.

2.5.2 Integration of Pressure in the Inlet Region

The integration of pressure in the inlet region is represented

by Eq. (30) and is rewritten below:

$$Q = -\left(16P_{HZ}V_o\right)\left\{\int_{-\infty}^{-X_{KI}}\left[\frac{1}{\bar{\rho}H^3}\frac{\partial(\ell n\ \bar{\mu})}{\partial P}\int_{-X}^{o}\frac{\partial(\bar{\rho}H)}{\partial T}\,dZ\right]dX\right.$$

$$\left.+\int_{-X_{KI}}^{-X_{KO}}\left[\frac{1}{\bar{\rho}H^3}\frac{\partial(\ell n\ \bar{\mu})}{\partial P}\int_{-X}^{o}\frac{\partial(\bar{\rho}H)}{\partial T}\,dZ\right]dX\right\} \qquad (30)$$

In the above equation the integral is split into two parts: the first in the integral over far left of the inlet region ($-\infty < X < -X_{KI}$) and the second is the remaining of the inlet region ($-X_{KI} < X < -X_{Ko}$).

We can approximate the integrand of the first integral,

$$\int_{-\infty}^{-X_{KI}}\left[\frac{1}{\bar{\rho}H^3}\frac{\partial(\ell n\ \bar{\mu})}{\partial P}\int_{-X}^{o}\frac{\partial(\bar{\rho}H)}{\partial T}\,dZ\right]dX = \int_{-\infty}^{-X_{KI}}\frac{X}{H_I^3}\frac{\partial(\ell n\ \bar{\mu})}{\partial P}\,dX \qquad (36)$$

where we assumed that

$$\bar{\rho} \cong 1,\quad H_I \cong 1 + 8P_{HZ}{}^2X^2 + D_{KI}\ ,\quad \frac{\partial(\bar{\rho}H)}{\partial T} \cong -1\ .$$

Since the pressure in the inlet region is not high, the normalized density is close to unity. D_{KI} is the deformation at $X = -X_{KI}$ which is the lower limit of the deformation integral. The deformation in this region is assumed to be constant. This assumption will not produce much error since the approach velocity due to the deformation is relatively a small term compared to the other

terms in the integrand.

Regardless of which viscosity model is used in the governing equation, the viscosity varies exponentially with pressure in the inlet region. Therefore, $\frac{\partial(\ell n\ \bar{\mu})}{\partial P} = \bar{\alpha}$.

Eq. (36) is integrated analytically,

$$\int_{-\infty}^{-X_{KI}} \frac{X}{H_I^3} \frac{\partial(\ell n\ \bar{\mu})}{\partial P}\, dX = \frac{\bar{\alpha}}{16 P_{HZ}^2 H_{KI}^2} \tag{37}$$

where $H_{KI} = 1 + 8P_{HZ}^2 X_{KI}^2 + D_{KI}$.

The integrated Q written at Kth grid point and time T_m is

$$Q_{K,m} = -\left(16P_{HZ}\right)(V_{o,m}) \left\{ \frac{-\bar{\alpha}}{16 P_{HZ}^2 H_{KI}^2} \right.$$

$$\left. + \int_{-X_{KI}}^{-X_K} \left[\frac{1}{\bar{\rho}_{K,m} H_{K,m}} \frac{\partial(\ell n\ \bar{\mu}_{k,m})}{\partial P} \int_{-X}^{o} \left(\frac{\partial(\bar{\rho}H)}{\partial T} \right)_m dZ \right] dX \right\} \tag{38}$$

Once the converged solution for the pressure in the middle region is obtained, the integrand in Eq. (38) is assumed to be known except density because the pressure distribution in the middle region plays the dominant role in determining film thickness and approach velocity. In the inlet region the normalized density can be approximated to unity for the first iteration. Applying the trapezoidal rule for the integration of Eq. (38), we obtain $Q_{K,m}$. Then $P_{K,m}$ in the inlet is determined from $Q_{K,m}$ as:

$$Q_{K,m} = 1 - \frac{1}{\mu_{K,m}}$$

$$= 1 - e^{-\alpha P_{K,m}} \qquad (39)$$

Thus the pressure equation in the inlet region is

$$P_{K,m} = -\frac{1}{\alpha} \ell n(1 - Q_{K,m}) \qquad (40)$$

2.5.3 Calculation of Deformation

The deformation for an arbitrary pressure distribution can not be determined by the straightforward numerical integration because the integrand in the deformation equation becomes singular at X = Z. Care must be exercised in the formulation of the numerical integral formula by which the singularity at X = Z can be removed.

The detailed derivation of the quadrature formula for the singular integral kernel is presented in Appendix A and the quadrature formula is written below,

$$\int_{-X_{KI}}^{O} P_m(Z) \ell n |Z - X_K| dZ = \sum_{j=1,3,5}^{KO-2} \left[P_{jm} K_1 \left(-X_K, -Z_j\right) \right.$$

$$\left. + P_{j+1,m} K_2 \left(-X_K, -Z_j\right) + P_{j+2,m} K_3 \left(-X_K, -Z_j\right) \right] \qquad (41)$$

where

$$K_1\left(-X_K, -Z_j\right) = \frac{1}{2\delta_j}\left(-3S_j - S_{j+2}\right) - \frac{\overline{S}_j}{3\delta_j^2} - u_j(\ell n|u_j| - 1) \tag{42}$$

$$K_2\left(-X_K, -Z_j\right) = \frac{2}{\delta_j}\left(S_j + S_{j+2}\right) + \frac{2\overline{S}_j}{3\delta_j^2} \tag{43}$$

$$K_3\left(-X_K, -Z_j\right) = \frac{1}{2\delta_j}\left(-S_j - 3S_{j+2}\right) - \frac{\overline{S}_j}{3\delta_j^2} + u_{j+2}(\ell n|u_{j+2}| - 1) \tag{44}$$

and

$$\delta_j = Z_j - Z_{j+1} \tag{45}$$

$$u_j = -Z_j - X_K \tag{46}$$

$$S_j = \frac{u_j^2}{2}\left(\ell n|u_j| - \frac{3}{2}\right) \tag{47}$$

$$S_j = u_j\left(S_j - \frac{u_j^2}{6}\right) - u_{j+2}\left(S_{j+2} - \frac{u_{j+2}^2}{6}\right) \tag{48}$$

Since the pressure profile is symmetrical about X = 0, the second half of the deformation integral can be approximated in the same form of Eq. (41) by changing $-Z_j$ to Z_j in K_1, K_2 and K_3, thus

$$\int_{-X_{KI}}^{X_{KI}} P_m(Z)\,\ell n|Z - X_K|\,dZ = \sum_{j=1,3,5}^{KO-2} \left\{P_{j,m}\left[K_1\left(-X_K, -Z_j\right) + K_2\left(-X_K, Z_j\right)\right]\right.$$

$$\left. + P_{j+1,m}\left[K_2\left(-X_K, -Z_j\right) + K_2\left(-X_K, Z_j\right)\right] + P_{j+2,m}\left[K_3\left(-X_K, -Z_j\right) + K_3\left(-X_K, Z_j\right)\right]\right\}$$

and following the above procedure we obtain

$$\int_{-X_{KI}}^{X_{KI}} P_m(Z)\,\ell n|Z|\,dZ = \sum_{j=1,3,5}^{Ko-2} \left\{ P_{j,m}\left[K_1\left(X_{Ko},-Z_j\right) + K_2\left(X_{Ko},Z_j\right) \right] \right.$$

$$+ P_{j+1,m}\left[K_2\left(X_{Ko},-Z_j\right) + K_2\left(X_{Ko},Z_j\right) \right]$$

$$\left. + P_{j+2,m}\left[K_3\left(X_{Ko},-Z_j\right) + K_3\left(X_{Ko},Z_j\right) \right] \right\} \qquad (50)$$

where $X_{Ko} = 0.$

For the convenience of differentiating $D_{K,m}$ with respect to $P_{j,m}$, K_1, K_2 and K_3 are rearranged in such way that $P_{j,m}$ has a single coefficient $R(-X_{K,} - Z_j)$:

$$R\left(-X_{K,} - Z_j\right) = S_1\left(-X_{K,} - Z_j\right) \qquad j = 1$$

$$= S_2\left(-X_{K,} - Z_{j-1}\right) \qquad \text{even } 2 \le j \le Ko - 1$$

$$= S_3\left(-X_{K,} - Z_{j-2}\right) + S_1\left(-X_{K,} - Z_j\right) \qquad \text{odd } 3 \le j \le Ko - 2$$

$$= S_3\left(-X_{K,} - Z_{j-2}\right) \qquad j = Ko \qquad (51)$$

where

$$S_n\left(-X_{K,}- Z_j\right) = K_n\left(-X_{K,}- Z_j\right) + K_n\left(-X_K, Z_j\right) - K_n\left(X_{Ko,}- Z_j\right)$$

$$- K_n\left(X_{Ko}, Z_j\right) \tag{52}$$

The final form of the deformation equation is

$$D_{K,m} = - C_3 \sum_{j=1,2,--}^{Ko} R\left(-X_{K,}- Z_j\right) P_{j,m} \tag{53}$$

where $C_3 = \dfrac{16P_{HZ}^{\ 2}}{\pi}$

2.5.4 Elastohydrodynamic Equation in the Middle Region

Eq. (28) written at Kth grid point and time T_m is

$$\left(\frac{\partial P}{\partial X}\right)_{K,m} = - \left(16P_{HZ}\right)\left(\frac{V_{o,m}\bar{\mu}_{K,m}}{\bar{\rho}_{K,m}H_{K,m}^3}\right) \int_{-X_K}^{\infty} \left(\frac{\partial(\rho H)}{\partial T}\right)_m dX \tag{54}$$

The derivative $\left(\dfrac{\partial(\bar{\rho}H)}{\partial T}\right)_{K,m}$ in Eq. (54) may be split into three terms and can be approximated by the Lagrangian three point quadrature as

$$\left(\frac{\partial(\bar{\rho}H)}{\partial T}\right)_{K,m} = - \bar{\rho}_{K,m} + H_{g_{K,m}}\left(\frac{\partial\bar{\rho}}{\partial T}\right)_{K,m} + \left(\frac{\partial(\bar{\rho}D)}{\partial T}\right)_{K,m}$$

$$= \omega_{m-2}\left[H_{g_{K,m}}\bar{\rho}_{K,m-2} + (\bar{\rho}D)_{K,m-2}\right] \tag{55}$$

$$+ \omega_{m-1}\left[H_{g_{K,m}} \quad \bar{\rho}_{K,m-1} + (\bar{\rho}D)_{K,m-1}\right]$$

$$+ \omega_{m}\left[H_{g_{K,m}} \bar{\rho}_{K,m} + (\bar{\rho}D)_{K,m}\right] - \bar{\rho}_{K,m} \qquad (55) \text{ cont.}$$

where

$$\omega_{m-2} = \frac{T_m - T_{m-1}}{(T_{m-2} - T_{m-1})(T_{m-2} - T_m)} \qquad (56)$$

$$\omega_{m-1} = \frac{T_m - T_{m-1}}{(T_{m-1} - T_{m-2})(T_{m-1} - T_m)} \qquad (57)$$

$$\omega_{m} = \frac{(T_m - T_{m-1}) + (T_m - T_{m-2})}{(T_m - T_{m-1})(T_m - T_{m-2})} \qquad (58)$$

and

$$H_{g_{K,m}} = H_{o,m} + 8P_{HZ}{}^{2}X_K{}^{2} \qquad (59)$$

The first two terms on the right hand side of Eq. (55) can be grouped together and expressed by $\gamma_m(-X_K)$ in which all the variables were determined in the previous time steps. Therefore, $\gamma_m(-X_K)$ is not a function of $P_{j,m}$.

After rearranging the integrand in Eq. (55) to a pressure dependent term and a pressure independent term, Eq. (55) may be

written as

$$\left(\frac{\partial(\rho H)}{\partial T}\right)_{K,m} = \gamma_m\left(-X_K\right) - \omega_m \rho_{K,m}\left[H_{g,K,m} + D_{K,m} - 1\right] \qquad (60)$$

Thus

$$\int_{-X_K}^{o}\left(\frac{\partial(\rho H)}{\partial T}\right)_{K,m} dX = \int_{-X_K}^{o}\gamma_m(-X)dX - \omega_m \int_{-X_K}^{o}\bar{\rho}_m\left[H_{g_m} + D_m - 1\right] dX$$

$$= \frac{1}{2}\sum_{i=K}^{Ko}\gamma_m\left(-X_i\right)\Delta X_i - \frac{1}{2}\omega_m \sum_{i=K}^{Ko}\bar{\rho}_{i,m}\left[H_{g_{i,m}} + D_{i,m} - 1\right]\Delta X_i \qquad (61)$$

where $\quad \Delta X_i = X_{i+1} - X_{i-1} \qquad K + 1 \le i \le Ko-1$

$$= X_{i+1} - X_i \qquad i = K,\ Ko$$

Substituting Eq. (53) for $D_{i,m}$ in Eq. (61) and rearranging

$$\int_{-X_{K+1/2}}^{o}\left(\frac{\partial(\rho H)}{\partial T}\right)_{K,m} dX = \frac{1}{2}\left\{\sum_{i=K+1/2}^{Ko}\left[\gamma_m\left(-X_i\right)\right.\right.$$

$$\left.\left. - \omega_m\bar{\rho}_{i,m}\left(H_{g_{i,m}} - 1\right)\right]\Delta X_i + \omega_m C_3 \sum_{j=1}^{Ko} L\left(-X_{K,} - Z_j\right) P_{j,m}\right\} \qquad (62)$$

where

$$L\left(-X_K, Z_j\right) = \sum_{i=K+1/2}^{Ko} \rho_{i,m} R\left(-X_i, - Z_j\right) \Delta X_i$$

The integral term and the deformation terms in Eq. (54) are replaced by Eqs. (62) and (52), respectively. The discretized form for Eq. (54) at $-X_{K+1/2}$ can thus be written as

$$\Psi_m\left(P_{K+1/2}\right) = \left(\frac{P_{K+1,m} - P_{K,m}}{\Delta X_K}\right) \left(\frac{1 + \dfrac{B\, P_{K+1/2,m}}{1 + A_1 P_{K+1/2,m}}}{\text{Exp}\left(\bar{\alpha}\, P_{K+1/2,m}\right)}\right)$$

$$\left(H_{g_{K+1/2,m}} - C_3 \sum_{i=1}^{Ko} R\left(-X_{K+1/2}, - Z_j\right) P_{j,m}\right)^3$$

$$-\left(8 P_{HZ} V_{o,m}\right) \left\{ \sum_{i=K+1/2}^{Ko} \left[\gamma_m\left(-X_i\right) - \omega_m \bar{\rho}_{i,m} \left(H_{g_{i,m}} - 1\right) \right] \Delta X_i \right.$$

$$\left. + \omega_m C_3 \sum_{j=1}^{Ko} L\left(-X_K, - Z_j\right) P_{j,m} \right\} \qquad (63)$$

Eq. (63) is one of the typical equations in the system equations. If $\Psi_m(P)$ is written at every mid point between grid spacings in the middle region, there are N equations with N unknown, $P_{K,m}$, where N is the number of grid points in the middle region.

Applying the Newton-Raphson technique to the system equations, we obtain

$$\left\{\Psi_m(P)\right\}^{(n)} + \left\{\Delta P_m\right\}^{(n+1)} \left[\Delta\cdot\Psi_m(P)\right]^{(n)} = 0 \tag{64}$$

where $\{\ \}$ and $[\ ]$ represent a column matrix and an N x N matrix, respectively, and $\Delta\cdot$ indicates partial derivative is to be taken with respect to P_m. n is the level of iteration.

From Eq. (64) we obtain

$$\left\{\Delta P_m\right\}^{(n+1)} = -\left[\Delta\cdot\Psi_m(P)\right]^{-1(n)} \cdot \left\{\Psi_m(P)\right\}^{(n)} \tag{65}$$

The right hand side of Eq. (65) is assumed to be known from the lower level iteration, and $\left\{\Delta P_m\right\}^{(n+1)}$ is defined as

$$\left\{\Delta P_m\right\}^{(n+1)} = \left\{P_m\right\}^{(n+1)} - \left\{P_m\right\}^{(n)} \tag{66}$$

The elements of the matrixes in Eq. (65) are detailed in Appendix B.

The center approach velocity and the load at time T_m are

$$V_{o,m} = \frac{-Q_o}{\left(16P_{HZ}\right)\left\{\dfrac{-\bar{\alpha}}{16P_{HZ}^2 H_{KI,m}^2} + \displaystyle\int_{-X_{KI}}^{\infty}\left[\frac{1}{\bar{\rho}_{K,m}H_{K,m}^3}\frac{\partial(\ell n\ \bar{\mu}_{K,m})}{\partial P}\int_{-X}^{\infty}\left(\frac{\partial(\bar{\rho}H)}{\partial T}\right)_m dZ\right] dX\right\}} \tag{67}$$

and

$$W_m = \frac{1}{4P_{HZ}^2}\int_{-X_{KI}}^{X_{KI}} P_m(X)dX \tag{68}$$

where

$$Q_o = 1 - e^{-\bar{\alpha}} \qquad \text{for the straight exponential lubricant}$$

and

$$Q_o = 1 - e^{-\{\bar{\alpha}P_s + \bar{\beta}(1-P_s)\}} \qquad \text{for the composite-exponential lubricant.}$$

The film thickness written at Kth grid point and time T_m is

$$H_{K,m} = 1 + 8P_{HZ}{}^2 X_K{}^2 + D_{K,m} \tag{69}$$

$$D_{K,m} = - C_3 \sum_{j=1,2,--}^{Ko} R\left(-X_{K,} - Z_j\right) P_{j,m} \tag{53}$$

2.5.5 Outline of Numerical Procedure

For the computational convenience, it is assumed that the center pressure is constant while the value of load varies as the cylinder approaches the flat surface from a high point. The calculations are performed to obtain the several series of the solutions in which each series represent the solutions at various center film thickness with a fixed center pressure.

The best approach to the problem is to obtain analytically the pressure distribution for a high center film thickness by neglecting the deformation term in the hydrodynamic equation, and

at each time step the center film thickness is reduced a certain amount and is kept constant.

Written below are the precedures of numerical calculation at each time step:

1) At the first time step analytically obtained pressure distribution is used as an initial guessed pressure. From the second time on, the initial guessed pressure is determined by linearly extrapolating the previous pressure distributions.

2) Using the initially guessed pressure distribution, the film thickness, density and viscosity are calculated. Then the approach velocity is determined from these values. We set up system equations (63) to obtain the pressure correction terms in the middle region. Once the pressure distribution in the middle region is corrected by $\{\Delta P_m\}$, the inlet pressure profile is determined by linear interpolation with the factor $P_{KA,m}^{(n+1)}/P_{KA,m}^{(n)}$ where $P_{KA,m}^{(n+1)}$ is obtained from the system equation. The film thickness is calculated using the newly obtained pressure.

3) If the converged solution for the pressure in the middle region is obtained, Eq. (38) is solved for the inlet pressure and the center approach velocity $V_{o,m}$ is determined by Eq. (67). Now the overall pressure distribution is checked for convergence. If it has converged, the load W_m is calculated by Eq. (68) and one moves to the

next time step. Otherwise, the above procedures (2) and (3) are repeated until the converged solution is obtained.

CHAPTER 3 - DISCUSSION OF RESULTS

3.1 Introduction

The results of the present study are presented as a series of curves for pressure, film thickness, load and approach velocity calculated at a prescribed center pressure and at successive reductions of the center film thickness.

The pressure and film profiles for various parameters at successive stages during a normal approach process are plotted for the left half of the contact region. The integrated load and the approach velocity during each normal approach are plotted against the center film thickness or the minimum film thickness.

3.2 Pressure Profiles

Shown on Fig. 1-3 to 1-13 are the series of the pressure profiles. Each figure displays the change in pressure with film thickness as the cylinder approaches the flat surface for a given center pressure. The range of the center pressures employed in the present study is from 2.5×10^4psi ($1.723 \times 10^8 N/m^2$) to 1.5×10^5psi ($1.034 \times 10^9 N/m^2$) which are typical maximum stresses encountered in concentrated contacts.

In general, the trend of change in pressure with respect to the center film thickness is qualitatively similar for all cases, namely, at high film thickness the pressure level decreases steadily throughout the contact region with decreasing film thickness until it reaches a stage when the integrated load becomes a minimum. After this stage the pressure in the middle region reverses its trend and begins

to rise, but the pressure in the inlet region still continuously decreases as the center film further decreases. In all cases, the pressure rise is confined within a small fraction of the Hertzian half-width, and it does not appear to reach the Hertzian semi-elliptical shape.

For the straight-exponential lubricant, the pressure-viscosity coefficient, $\bar{\alpha}$, has a marked influence upon the pressure gradient near the center of the contact. For example, Fig. 1-9 shows that the pressure gradient for $\bar{\alpha} = 12.8$ at the center is far steeper than that appearing in Fig. 1-5 for $\bar{\alpha} = 9.5$.

The change in the center pressure also produces a very strong effect upon the pressure gradient at the center. A higher center pressure produces a sharper pressure spike at the center. The effect becomes increasingly stronger at higher center pressures. For example, at center pressure equal to 150,000 psi ($1.034 \times 10^9 N/m^2$), the pressure gradient gradually tends to become infinite. The existence of such sharp pressure spikes in practice appears to be highly questionable, since the shear stress would also become incredibly large under these circumstances. It appears very unlikely that the fluid can withstand such high shear stresses, particularly in the light of recent work on traction studies [10], [11], and [12] which demonstrate the existence of a limiting shear stress for any lubricant. In the vicinity of this limiting shear stress, the fluid behaves in a non-Newtonian fashion, and an increase in shear rate has little effect on the shear stress.

The effect of the non-Newtonian behavior can be accounted for indirect-

ly by introducing the so-called composite-exponential model for the lubricant viscosity. This was demonstrated by Allen et al [7] in a spinning torque study. The resulting pressure profiles using a composite-exponential model similar to that in [7] are shown in Fig. 1-10 to 1-13. These curves show considerably different features compared to the pressure curves for a straight exponential lubricant. For example, the pressure gradient is much more moderate near the contact center, showing the absense of a pressure spike which is so characteristic for the straight exponential lubricant. Moreover, the steepness of the pressure gradient near the contact center is not influenced greatly by the increase in the center pressure. For example, there is very little difference in the pressure gradient between Fig. 1-10 and Fig. 1-13 at the same film thickness.

It should be emphasized that the results for the composite-exponential lubricant are intended to show the qualitative effect of the reduction of pressure-viscosity coefficient on the characteristics of pressure and film profiles. These results should not be used quantitatively for design purposes.

3.3 Film Thickness

The film thickness profiles are plotted in conjunction with the corresponding pressure profiles in Fig. 1-3 to 1-13. At the early stage of normal approach, a pocket is formed elastically at the contact center, and its shape does not change much for subsequent reductions of the center film thickness. The pocket depth defined as the difference between the center film thickness H_o and the minimum film thickness, is depen-

dent upon the center pressure for a given lubricant. A higher center pressure produces a deeper pocket.

When the center film thickness decreases to a certain level, a quite different phenomenon occurs. At this point, the normal approach velocity at the center suddenly drops almost to zero, while the local approach velocity elsewhere in the contact continues. This condition produces a deeper pocket during the final stages of the normal approach. In all cases investigated, the growth of the pocket persists all the way down to the very end when the edge of the contact at the minimum film thickness point practically touches the opposing surface. For perfectly smooth surfaces, the point of the minimum film would eventually form a seal and the lubricant inside this point would be trapped. Thus, by including the local approach velocity in the analysis, one can show that both the pressure and film thickness profiles never reach the semi-elliptical Hertzian shape as suggested by Christensen in [4]. Instead, the pressure remains to be confined in the center region, and the surface deformed into a pocket inside which a portion of the lubricant is entrapped. As shown in these deformation shapes, the center pressure has a definite influence upon the depth as well as the width of the pocket. In general, the pocket becomes deeper and wider as the center pressure increases.

The pocket formation is more pronounced for the case of the composite exponential lubricant. The pocket depth is somewhat greater than the corresponding case for the straight exponential lubricant. The change of the pocket shape during normal approach is qualitatively similar to that for the straight exponential lubricant. At the last

time step when the minimum film thickness H, is less than 5×10^{-6} the pocket depth increases rapidly while the location of the minimum film thickness moves slightly toward the outer edge of the contact region. The highest value of pocket depth for all cases investigated occurs at a center pressure, $P_o = 1.5 \times 10^5$ psi ($1.034 \times 10^9 N/m^2$), with the composite exponential lubricant. The value of the maximum depth exceeds 30×10^{-6}, and there is practically no significant pressurization outside of the pocket. It is thus expected that during the normal approach of two cylinders the pressurization is effectively contained inside the pocket and that the width of the pocket is approximately one-half of the Hertzian contact width based on the same center pressure.

3.4 Load

Shown on Fig. 1-14 are the load vs. center film thickness curves at a constant center pressure for the straight-exponential lubricant. In general, the dependence of load on the pressure-viscosity coefficient $\bar{\alpha}$ and the center pressure in the present analysis confirms Christensen's conclusions: first, for a given center pressure, the load is strongly dependent upon the pressure viscosity coefficient, i.e., the higher $\bar{\alpha}$ produces much smaller load. For example, the load for $\bar{\alpha} = 12.8$ and $P_o = 100{,}000$ psi ($6.894 \times 10^8 N/m^2$) is approximately equal to the load for $\bar{\alpha} = 9.8$ and $P_o = 25{,}000$ psi ($1.723 \times 10^8 N/m^2$); and second, once the center pressure is sufficiently high, the increase in load is negligibly small for further increase in center pressure, i.e., the load becomes insensitive to the center pressure. As described

before in Section 3.2, this insensitivity of load to the increase in center pressure is caused by a strong pressure-viscosity coefficient $\bar{\alpha}$. Thus, one would expect that if the increase in viscosity with pressure is milder, the load becomes more dependent upon the center pressure, as will be seen in the results of the composite-exponential lubricant.

Also in Fig. 1-15, a quantitative comparison is made between the load curves obtained by Christensen [4] and those calculated from the present analysis. On the right side of the minimum load, the two theories shows fairly close agreement, the present analysis yielding a slightly higher load. This slight discrepancy in load is attributable to two effects: first, the approach velocity in the present analysis is higher than that in [4] where the local deformation velocity is neglected, resulting in stronger squeezing action on the fluid by the cylinder, and second, the effect of the compressibility of the lubricant, which was also neglected in [4]. On the left side of the minimum load, the effect of the local deformation velocity becomes very important, and the present theory gives considerably higher load than Christensen's results. Furthermore, there is also considerable difference in slope between the two results. The present theory predicts a much steeper slope on the left side of the minimum load, indicating that there is virtually no reduction in the center film thickness while the minimum film thickness steadily drops to zero as shown on Fig. 1-15.

It should be noted that the maximum load obtained in the present analysis is substantially less than the corresponding Hertzian load based on the same center pressure. This result directly contradicts

Christensen's conclusion that the load increases to the Hertzian load as the minimum film thickness decreases to zero.

As shown on Fig. 1-18, one may find the variation of center pressure at a constant load during the normal approach of the two cylinders from Fig. 1-15 and 1-17. If a horizontal straight line is drawn at any specific load on Fig. 1-15 or Fig. 1-17, depending upon the lubricant used, the change in P_o with decreasing center film thickness can be determined from the intersection of the straight line and load curve. The center pressure gradually increases with decreasing center film thickness, and then increases abruptly to the maximum value; the maximum is much larger than the initial p_o. The center pressure finally decreases rapidly for further decrease in center film thickness.

In Figs. 16 and 17, results of the composite-exponential lubricant show that in general, the loads are much larger than the corresponding loads for the straight-exponential lubricant. The change in load with the center film thickness, or with the minimum film thickness, is somewhat moderate. No abrupt increase in load is seen. The most noticeable effect produced by the composite-exponential lubricant is the relationship between load and center film thickness. The load is strongly dependent upon the center pressure.

3.5 Approaching Velocity

As mentioned in Section 2.2.3, the center approach velocities shown on Fig. 1-19 are not the absolute velocities - the

velocities of the approaching cylinder center they are the relative center approach velocities, i.e., the time derivative of the center film thickness. However, it is known that in the normal approach problem of EHD lubrication the difference between them is negligibly small.

It is apparent from Fig. 1-19 that the center approach velocity V_o decreases with decreasing center film thickness at a constant center pressure, and the rate of reduction in V_o is a function of H_o and P_o. In the region of high H_o, the center approach velocity approximately varies with the square of the center film thickness for a given center pressure. This trend agrees with that predicted by the normal approach solution between two rigid cylinders. This parabolic relation between H_o and V_o ceases to exist as H_o is reduced to a certain value depending upon P_o. For example, for $P_o = 1.25 \times 10^5$ psi ($8.617 \times 10^8 N/m^2$) and H_o approaching 3×10^{-5}, V_o decreases rapidly for further decrease in H_o. For low center pressure, this transition occurs at a much smaller value of H_o. The rapid reduction of the center approach velocity for high center pressure can be explained by considering the flow quantity through the gap between the bump and the flat surface. The gap is not more than 10 microinches so that the lubricant flow through this gap is very small; consequently very little squeezing on the lubricant is necessary to maintain a constant P_o.

It is interesting to note that the center velocity V_o required to produce a high center pressure P_o at a constant center film thickness H_o is considerably lower than that for a lower P_o. This trend directly opposes that based on the rigid cylinder theory for which a greater

P_o requires a high center velocity V_o at a same center film thickness H_o. This discrepancy can be accounted for by the deformation effect. At a higher pressure, the contact region is larger, the squeezing action is thus much more effective; and it requires a smaller center velocity to produce the required center pressure.

Fig. 1-20 shows the ratio of local approach velocity to center approach velocity vs. H/W for three points of the contact region X = -0.25, -0.5 and -0.75. For the sake of comparison, typical data from [5] are also shown on Fig. 1-20. As expounded in Section 2.2.3, it is known that local approach velocity varies along the contact surface and the most severe variation occurs when the film thickness is very small. The data from [5] is based on the assumption of iso-viscous lubricant, which shows the variation of local velocity is relatively small compared with that for the lubricant of variable viscosity. This comparison clearly indicates that it is much more difficult, sometimes almost impossible, to obtain the converged solution when the center film thickness is small because controlling the local velocity numerically between two successive iterations is very difficult.

CHAPTER 4 - SUMMARY OF RESULTS

It has been found that the full solution of the normal approach problem of two elastic cylinders, with a compressible lubricant between them whose viscosity varies exponentially with pressure, can be obtained by solving numerically the coupled transient Reynolds equation and the elasticity equation using a combination of direct iteration and Newton-Raphson method.

The results show that:

1) In general, the pressure profile for the straight exponential lubricant shows a sharp spike near the contact center; a higher center pressure or a higher pressure-viscosity coefficient results in a steeper pressure profile at the contact center. However, for the case of the composite-exponential lubricant the steepness of the pressure profile at the contact center does not depend so strongly upon the center pressure.

2) For all cases studied, a pocket is formed elastically on the cylinder surface near the contact center during the early stage of the normal approach, and it remains without much change in its shape until the final stages of the normal approach, resulting in a quantity of lubricant inside the pocket being entrapped. Thus, the film profile never reaches the semi-elliptical Hertzian shape as suggested by Christensen [4]. The depth of the pocket is dependent upon the center pressure for all cases investigated. In comparison, the pocket depth for the composite-exponential lubricant is much deeper than the corresponding one for the

straight-exponential lubricant.

3) In general, the load increases very rapidly from its minimum value with virtually no reduction in the center film thickness. This result can be attributed to the fact that the entrapped lubricant inside the pocket is effectively pressurized further by closing the gap between the minimum film thickness and the flat surface. This pressurization, in turn, deepens the pocket depth further. Thus, for all cases investigated, the load never increases to the Hertzian load based on the same center pressure as the minimum film thickness decreases to zero. In contrast to the cases for the straight exponential lubricant where for a sufficiently high center pressure and at any given center film thickness the load is insensitive to the center pressure, the load fo the composite-exponential lubricant is strongly dependent upon the center pressure.

4) At early stages of the normal approach, the local approach velocity does not deviate from the center approach velocity. However, during the final stages, the ratio of local velocity to center velocity greatly exceeds unity, indicating that the center film thickness is almost constant while the film elsewhere continuously decreases. For a given center film thickness, the center approach velocity required to produce a higher center pressure is considerably lower than that for a lower pressure. This trend is more pronounced at the final stages of the normal approach when the deformation overtakes the geometrical film thickness.

APPENDIX A

QUADRATURE FOR INTEGRATION OF ELASTICITY EQUATION*

Referring to [13] for detailed derivation, the normal displacement for any x on the surface of semi-infinite solid due to vertical forces is given by

$$D_m(X) = \int_{-X_{KI}}^{X_{KI}} P_m(Z) \ln \frac{|Z - X|}{|Z|} dZ \qquad (A.1)$$

where the symbol $|Z - X|$ represents the positive distance between the force element at Z and the point of interest at X as shown on Fig. A-1.

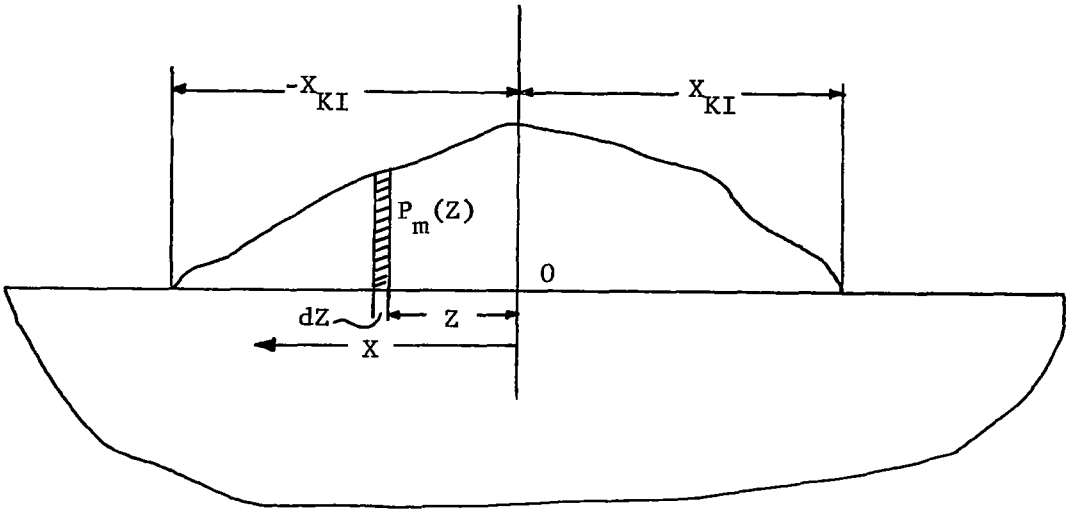

Fig. A-1

Since the integrand is singular at X = Z, the numerical quadrature formula should be developed in such a way that the singularity at X = Z can be removed. It consists of approximating the function P by a parabolic polynomial in each subinterval, performing the integration in closed form in the subinterval, and summing over the whole region of integration.

We subdivide the right half of the contact region into N subintervals, requiring that the widths of two consecutive subintervals equal and assuming the pressure distribution is known. Then

$$I(X) = \int_{o}^{X_{KI}} P_m(Z) \ell n |Z - X_K| dZ = \sum_{j=1}^{N} I_j(X) \tag{A.2}$$

where

$$I_j(X) = \int_{Z_j}^{Z_{j+1}} P_m(Z) \ell n |Z - X_K| dZ \tag{A.3}$$

The parabolic representative of the pressure distribution in the subinterval $[Z_j, Z_{j+1}]$ is

$$P_m(Z) = \Big[\left(Z - Z_{j+1/2}\right)\left(Z - Z_{j+1}\right) P_{j,m} - 2\left(Z - Z_j\right)\left(Z - Z_{j+1}\right) P_{j+1/2,m}$$

$$+ \left(Z - Z_j\right)\left(Z - Z_{j+1/2}\right) P_{j+1,m} \Big] / 2\Delta_j^2 \tag{A.4}$$

where

$$P_{K,m} = P_m\left(Z_K\right)$$

$$\Delta_j = \frac{1}{2}\left(Z_{j+1} - Z_j\right)$$

From (A.4),

$$P'_{j,m} = P'_m(Z_j) = \left(-3P_{j,m} + 4P_{j+1/2,m} - P_{j+1,m}\right)/2\Delta_j,$$

$$P'_{j+1,m} = P'_m(Z_{j+1}) = \left(P_{j,m} - 4P_{j+1/2,m} + P_{j+1,m}\right)/2\Delta_j,$$

$$P''_{j,m} = P''_{j+1,m} = \left(P_{j,m} - 2P_{j+1/2,m} + P_{j+1,m}\right)/\Delta_j^2 \qquad \text{(A.5)}$$

We integrate Eq. (A.3) by parts several times to obtain

$$I_j(X) = \left[P_m(Z)D_f^{-1}\left\{\ell n|Z - X|\right\} - P'_m(Z)D_f^{-2}\left\{\ell n|Z - X|\right\} + P''_m(Z)D_f^{-3}\left\{\ell n|Z - X|\right\}\right]_{Z_j}^{Z_{j+1}} \qquad \text{(A.6)}$$

where

$$D_f^{-1}\left\{\ell n|Z - X|\right\} = \int \ell n|Z - X|dZ$$

$$D_f^{-2}\left\{\ell n|Z - X|\right\} = \iint \ell n|Z - X|\, dZ$$

$$D_f^{-3}\left\{\ell n|Z - X|\right\} = \iiint \ell n|Z - X|dZ \qquad \text{(A.7)}$$

Thus

$$D_f^{-1}\left\{\ell n|Z - X|\right\} = (Z - X)\ell n|Z - X| - (Z - X)$$

$$D_f^{-2}\left\{\ell n|Z - X|\right\} = \frac{1}{2}(Z - X)^2 \ell n|Z - X| - \frac{3}{4}(Z - X)^2 \qquad \text{(A.8)}$$

$$D_f^{-3}\left\{\ell n|Z - X|\right\} = \frac{1}{6}(Z - X)^3 \ell n|Z - X| - \frac{11}{36}(Z - X)^3 \qquad \text{(A.8) cont.}$$

Substituting (A.8) in (A.6) and some manipulation yields

$$I_j(X) = \Big[(Z - X)\left\{\ell n|Z - X| - 1\right\}\left\{P_m(Z) - \frac{1}{2}(Z - X)P'_m(Z) + (Z - X)^2 P''_m(Z)/6\right\}$$

$$+ (Z - X)^2 P'_m(Z) - 5(Z - X)P''_m(Z)/9\Big\}/4\Big]_{Z_j}^{Z_{j+1}} \qquad \text{(A.9)}$$

Let $u_j = Z_j - X_K$, $u_{j+1} = Z_{j+1} - X$ and $\mathbf{S}_j = \frac{1}{2} u_j^2\left[\ell n|u_j| - \frac{3}{2}\right]$ with these variables and noting that at the end points of each sub-interval in the interior of $[-X_{KI}, 0]$, there is exact cancellation of the $P_m(Z)$ contribution, Eq. (A.9) is rewritten as:

$$I_j(X_K) = \left(P_{j,m}S_j - P'_{j+1,m}S_{j+1}\right) - \frac{1}{3}P''_m\Big[u_j\left(S_j - \frac{1}{6}u_j^2\right)$$

$$- u_{j+1}\left(S_{j+1} - \frac{1}{6}u_{j+1}^2\right)\Big] \qquad \text{(A.10)}$$

Substituting Eq. (A.5) for P' and P'' in (A.10) and summing over the entire interval. We obtain,

$$\int_o^{X_{KI}} P_m(Z)\ell n|Z - X_K|dZ = \sum_{1,3,5}^{N-2}\Big[P_{j,m}K_1(X_K, Z_j) + P_{j+1,m}K_2(X_K, Z_j)$$

$$+ P_{j+2,m}K_3(X_K Z_j)\Big] \qquad \text{(A.11)}$$

where

$$K_1(X_K, Z_j) = -\frac{1}{2\delta_j}\left(3S_j + S_{j+2}\right) - \frac{\bar{S}_j}{3\delta_j^2} - u_j\left[\ln|u_j| - 1\right],$$

$$K_2(X_K, Z_j) = \frac{2}{\delta_j}\left(S_j + S_{j+2}\right) + \frac{2\bar{S}_j}{3\delta_j^2},$$

$$K_3(X_K, Z_j) = \frac{1}{2\delta_j}\left(-S_j - 3S_{j+2}\right) - \frac{\bar{S}_j}{3\delta_j^2} + u_{j+2}\left[\ln|u_{j+2}| - 1\right],$$

and

$$\bar{S}_j = u_j\left(S_j - \frac{1}{6}u_j^2\right) - u_{j+2}\left(S_{j+2} - \frac{1}{6}u_{j+2}^2\right).$$

---

* The quadrature formulation for the singular kernel in the integrand written here is exactly the same as that of Ref. [14].

APPENDIX B

CALCULATION OF MATRIX ELEMENTS IN EQ. (64)

For convenience, Eq. (63) and (64) are rewritten below

$$\Psi_m\left(P_{K+1/2}\right) = \left(\frac{P_{K+1,m}-P_{K,m}}{\Delta X_K}\right)\left(\frac{1+\dfrac{BP_{K+1/2,m}}{1+A_1P_{K+1/2,m}}}{EXP\left(\bar{\alpha}\,P_{K+1/2,m}\right)}\right)$$

$$\left(H_{g_{K+1/2,m}} - C_3\sum_{j=1}^{KO} R\left(-X_{K+1/2,}-Z_j\right)P_{j,m}\right)^3$$

$$-\left(8P_{HZ}V_{o,m}\right)\left\{\sum_{i=K+1/2}^{KO}\left[\gamma_m(-X_i) - \omega_m\bar{\rho}_{i,m}\left(H_{g_{i,m}}-1\right)\right]\Delta X_i\right.$$

$$\left. + \omega_m C_3\sum_{j=1}^{KO} L\left(-X_{K,}-Z_j\right)P_{j,m}\right\} \qquad (63)$$

$$\left\{\Psi_m(P)\right\} + \left\{\Delta P_m\right\}\left[\Delta\cdot\Psi_m(P)\right] = 0 \qquad (64)$$

The calculation of the matrix elements in $[\Delta\cdot\Psi_m(P)]$ involves the differentiation of $\{\Psi_m(P)\}$ with respect to $\{P_m\}$. Before differentiation, Eq. (63) is rewritten in the following form:

$$\Psi_m(P_{K+1/2}) = \frac{1}{8}\left(\frac{P_{K+1,m}-P_{K,m}}{\Delta X_K}\right)\left(\frac{\bar{\rho}_{K+1/2,m}}{\bar{\mu}_{K+1/2,m}}\right)\left(H_{K+1,m}+H_{K,m}\right)^3$$

$$-\left(4P_{HZ}V_{o,m}\right)\left(I_{K+1,m}+I_{K,m}\right) \qquad (B.1)$$

where

$$I_K = \sum_{i=K}^{KO} \left[\gamma_m(-X_i) - \omega_m \bar{\rho}_{i,m} \left(H_{g_{i,m}} - 1\right)\right] \Delta X_i + \omega_m C_3 \sum_{j=1}^{KO} L\left(-X_K, -Z_j\right) P_{j,m} \tag{B.2}$$

and

The variables, $H_{K+1/2,m}$ and $I_{K+1/2,m}$, are expressed as the average of the two values at $-X_K$ and $-X_{K+1}$ as:

$$I_{K+1/2,m} = \frac{1}{2}\left(I_{K+1,m} + I_{K,m}\right) \tag{B.3}$$

$$H_{K+1/2,m} = \frac{1}{2}\left(H_{K+1,m} + H_{K,m}\right) \tag{B.4}$$

The $\bar{\rho}_{K+1/2,m}$ and $\bar{\mu}_{K+1/2,m}$ are taken as a function of the average pressure, $\frac{1}{2}\left(P_{K+1,m} + P_{K,m}\right)$ and expressed below:

$$\bar{\rho}_{K+1/2,m} = \frac{\frac{1}{2} B \left(P_{K+1,m} + P_{K,m}\right)}{1 + \frac{1}{2} A_1 \left(P_{K+1,m} + P_{K,m}\right)} \tag{B.5}$$

$$\bar{\mu}_{K+1/2,m} = \exp\left[\frac{1}{2} \bar{\alpha} \left(P_{K+1,m} + P_{K,m}\right)\right] \tag{B.6}$$

The derivative of the variables in $\Psi_m(P_{K+1/2})$ are derived below:

$$\frac{\partial I_{K,m}}{\partial P_{j,m}} = \omega_m C_3 L(-X_K, - Z_j) - (\delta_s)(\omega_m \Delta X_K) \left(\frac{\partial \bar{\rho}}{\partial P}\right)_{K,m} (H_{K,m} - 1) \tag{B.7}$$

where

$$\delta_s = 1 \qquad \text{for } j \geq K$$

$$\delta_s = 0 \qquad \text{for } j < K$$

and

$$\text{if } j \neq KA,\ L(-X_{K,} - Z_j) = \sum_{i=K}^{K0} \bar{\rho}_{i,m} R(-X_{i,} - Z_j) \Delta X_i$$

$$\text{if } j = KA,\ L(-X_{KA,} - Z_j) = \sum_{i=KA}^{K0} \sum_{j=1}^{KA} \rho_{i,m} R(-X_{i,} - Z_j) \left(\frac{P_{i,m}}{P_{KA,m}}\right) \Delta X_i$$

In this way, we can take into account the effect of the pressure distribution in the inlet region on $D_{KA,m}$ - the deformation at the dividing point between the inlet and middle region, since $D_{KA,m}$ is strongly dependent upon the inlet pressure distribution.

If $j = K$ or $K + 1$, then

$$\frac{\partial \bar{\mu}_{K+1/2,m}}{\partial P_{j,m}} = \frac{\partial}{\partial P_{j,m}} \left(\exp\left[\frac{1}{2} \bar{\alpha} \left(P_{K+1,m} + P_{K,m} \right] \right) \right)$$

$$= \frac{1}{2} \bar{\alpha}\, \bar{\mu}_{K+1/2,m} \tag{B.8}$$

$$\frac{\partial \bar{\rho}_{K+1/2,m}}{\partial P_{j,m}} = \frac{\partial}{\partial P_{j,m}} \left\{ 1 + \frac{\frac{1}{2} B \left(P_{K+1,m} + P_{K,m} \right)}{1 + \frac{1}{2} A_1 \left(P_{K+1,m} + P_{K,m} \right)} \right\}$$

$$= \frac{B}{2 + A_1 \left(P_{K+1,m} + P_{K,m} \right)} \tag{B.9}$$

Since the deformation, $D_{K,m,}$ depend upon the overall pressure distribution, the derivative of $D_{K,m}$ with respect to any $P_{j,m}$ exists.

Thus

$$\frac{\partial H^3_{K+1/2,m}}{\partial P_{j,m}} = -\left(3\ C_3 RR_{K,j}\right)\left(H_{K+1,m} + H_{K,m}\right) \qquad \text{(B.10)}$$

where

$$RR_{K,j} = R\left(-X_{K+1,} - Z_j\right) + R\left(-X_{K,} - Z_j\right) \qquad \text{for } j \neq KA,\ KA+1$$

$$RR_{K,j} = \sum_{i=1}^{KA}\left\{\left[R\left(-X_{K+1,} - Z_i\right) + R\left(-X_{K,} - Z_i\right)\right]\left(\frac{P_{i,m}}{P_{KA,m}}\right)\right\} \text{ for } j = KA,\ KA+1$$

The reason for summing the products of the deformation kernel and the inlet pressure ratio over the entire grid in the inlet region is to take into account the effect of the inlet pressure distribution on $D_{KA,m} + D_{KA+1,m}$.

Using Eqs. (B.7), (B.8), (B.9) and (B.10), the derivative of $\Psi_m(P_{K+1/2})$ is written as:

$$\frac{\partial \Psi_m(P_{K+1/2}}{\partial P_{j,m}} = -\left(\frac{3}{8}\ C_3\right)\left(RR_{K,j}\right)\left(H_{K+1,m} + H_{K,m}\right)^2\left(\frac{\bar{\rho}_{K+1/2,m}}{\bar{\mu}_{K+1/2,m}}\right)\left(\frac{P_{K+1,m} - P_{K,m}}{\Delta X_K}\right)$$

$$-\left(4\ P_{HZ} V_{o,m}\right)\left\{\left[\omega_m C_3\left[L\left(-X_{K,} - Z_j\right) + L\left(-X_{K+1,} - Z_j\right)\right] - \left(\delta_s \omega_m\right)\right.\right.$$

$$\left.\left(\frac{B}{2 + A_1\left(P_{K+1,m} + P_{K,m}\right)}\right)\left[\left(H_{K,m} - 1\right)\left(\Delta X_K\right) + \left(H_{K+1,m} - 1\right)\left(\Delta X_{K+1}\right)\right]\right\}$$

$$+ \left(\delta_u\right)\frac{\left(H_{K+1,m} + H_{K,m}\right)^3}{8\Delta X_K}\left\{\left(P_{K+1,m} - P_{K,m}\right)\left[\frac{\bar{\mu}_{K+1/2,m} B}{2 + A_1\left(P_{K+1,m} + P_{K,m}\right)}\right.\right. \qquad \text{(B.11)}$$

$$+ \left(\frac{\bar{\rho}_{K+1/2,m}}{\bar{\mu}_{K+1/2,m}}\right)\left(\frac{\alpha}{2}\right)\Big] - \left(\frac{\bar{\rho}_{K+1/2,m}}{\bar{\mu}_{K+1/2,m}}\right)\left(\delta_g\right)\Big\} \qquad \text{(B.11) cont.}$$

where

$$\delta_u = 0 \qquad j \neq K,\ K+1,$$

$$\delta_u = 1 \qquad j \neq K,\ K+1,$$

and

$$\delta_g = 1 \qquad j = K+1,$$

$$\delta_g = -1 \qquad j = K\ .$$

Eq. (B.11) is one of the typical matrix elements. The expanded form of Eq. (64) is

$$\begin{bmatrix} \frac{\partial \Psi_m(P_{KA})}{\partial P_{KA,m}}, & \frac{\partial \Psi_m(P_{KA})}{\partial P_{KA+1,m}}, & \cdots & \frac{\partial \Psi_m(P_{KA})}{\partial P_{K0-1,m}}, \\ \frac{\partial \Psi_m(P_{KA+1})}{\partial P_{KA,m}}, & \frac{\partial \Psi_m(P_{KA+1})}{\partial P_{KA+1,m}}, & \cdots & \frac{\partial \Psi_m(P_{KA+1})}{\partial P_{K0-1,m}}, \\ \vdots & \vdots & & \vdots \\ \frac{\partial \Psi_m(P_{K0-1})}{\partial P_{KA,m}}, & \frac{\partial \Psi_m(P_{K0-1})}{\partial P_{KA+1,m}} & \cdots & \frac{\partial \Psi_m(P_{K0-1})}{\partial P_{K0-1,m}}, \end{bmatrix} \begin{bmatrix} \Delta P_{KA,m} \\ \Delta P_{KA+1,m} \\ \vdots \\ \Delta P_{K0-1,m} \end{bmatrix} = \begin{bmatrix} \Psi_m(P_{KA}) \\ \Psi'_m(P_{KA+1}) \\ \\ \Psi_m(P_{K0-1}) \end{bmatrix}$$

(B.12)

The pressure correction term at the contact center, $\Delta P_{KO,m}$, is not necessary since the center pressure is assumed to be constant. The center velocity $V_{o,m}$ is kept constant during the calculation of the pressure correction terms. The center velocity is recalculated after the converged solution for the pressure distribution in the middle region is obtained.

APPENDIX C

COMPUTER PROGRAM FLOW DIAGRAM AND FORTRAN LISTINGS

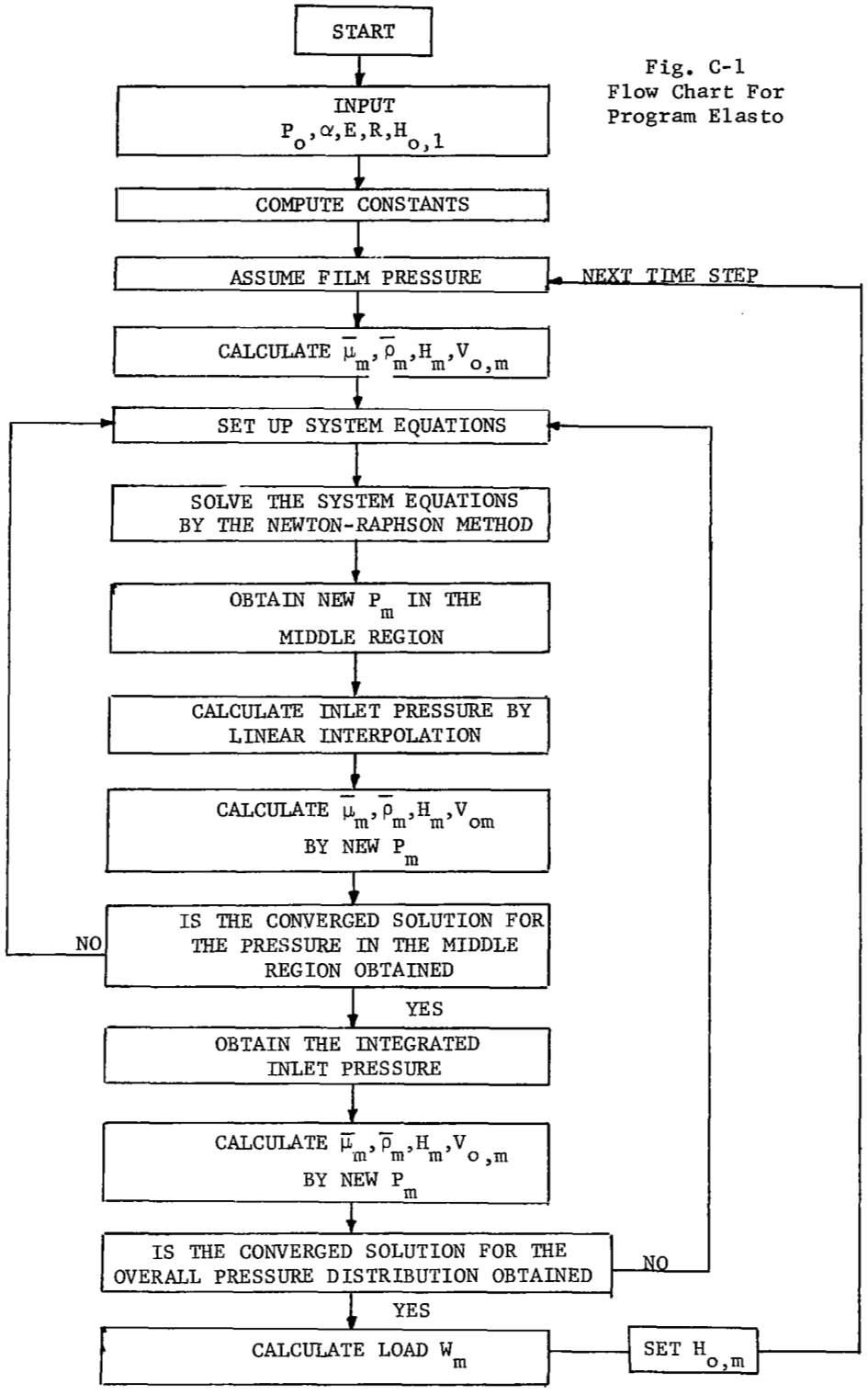

Fig. C-1
Flow Chart For
Program Elasto

```
      PROGRAM ELASTO (INPUT, OUTPUT, PUNCH, TAPE5=INPUT, TAPE6=OUTPUT)
      COMMON/A/KF, ALPH, EN, ED, HE, HE1, ALPH1, MM
      COMMON KI, KA, KKI, KKF, KF2, KF3, V, KKE, IS, N, NN, PO, K, M,
     1PM, PC, KS, EP, EU, W, WW, MM, RA, KO, PNR, PDI, XH, DX, DI, D,
     2HG,H,P,VIS,VISD,DEN,DEND,T,DT,VD,DP,HO,SE,A,B,C,SD,AM,PS,
     3OMEG3,OMEG2,OMEG1,DENT,DD,DS,C4,C5,II,Q,PAI,BET,P1,P2,VIS1,
     4VIS2,VIS3,DPV,C6,EBF,SUBV,CC,EE,PKA,DPR,R
      DIMENSION XH(51),DX(51),D(51,3),HG(51,3),H(51,3),DI(51),
     1P(51,3),VIS(51),VISD(51),DEN(51,3),DEND(51,3),T(35),V(35),
     2DT(35),VD(51),DP(51),HO(50),W(35),SE(51),A(51),B(51),CC(51),
     3F(51),R(51,51),BET(51,51),SD(51),PS(51),OMEG3(3),OMEG2(3),
     4OMEG1(3),DENT(51),Q(51,51),PAI(51),SUBV(51),C(2,3,51),EE(51)
      DIMENSION TEM(51),NI(51,4)
      READ(5,200) KI, KF, MI, MF, ED, EN, ALPH, PH
      READ(5,203) EP, EU, HO1, RA
      READ(5,206) (XH(K), K=KI,KF)
      READ(5,205) ((Q(K,J), J=KI,KF), K=KI, KF)
      KKI=KI+1
      KF2=KF-2
      NG=3
      KF3=1
      KKF=KF-1
      E=33.6E+6
      HO1=200.0E-6
      EN=EN*1.25$ED=ED*1.25$ALPH=ALPH*1.25$PH=125000.0
      WRITE(6,217) ED, EN, ALPH, PH
      WRITE(6,841) (K,XH(K),K=KI,KF)
      NI=2 $ NI=3
      KA=35
      PHZ=PH/E
      C4=16.0*PHZ $ C5=C4*PHZ $ C6=C5/3.14
      WRITE(6,205) PHZ, C4, C5, C6, E
      IF(NT.EQ.1) 27, 39
   27 READ(5,205) (P(K,2),K=KI,KF)
      READ(5,205) (P(K,1), K=KI, KF)
      READ(5,231) H(KA,1),T(1)
      READ(5,231) H(KA,2), T(2)
      II=2 $ IS=2 $ MM=1 $ M=1 $ CALL DVD $ CALL HDT
      MM=1 $ IS=2 $  M=2 $ CALL DVD $ CALL HDT
      WRITE(6,668) (K, P(K,2), K=KI, KF)
      WRITE(6,206) H(KA,1), T(1)
      WRITE(6,206) H(KA,2), T(2)
      WRITE(6,668) (K, H(K,1), K=KI, KF)
      WRITE(6,668) (K, H(K,2), K=KI, KF)
      WRITE(6,668) (K, D(K,1), K=KI, KF)
      WRITE(6,668) (K, D(K,2), K=KI, KF)
      CALL INTEG1(XH(KI),XH(KF),2,P(1,2),KF,VALUE,IER)
      DO 394 K=KI, KKF
  394 DX(K)=XH(K+1)-XH(K)
      ALPH1=ALPH*0.5
   39 DO 37 K=KI,KF
   37 B(K)=ALPH
      AP=1.0-(1.0/EXP(ALPH))
      A(KF)=AP
      DO 50 MM=1,35
      KF3=2
      KA1=KA-1
      IF(MM-2) 83, 56, 57
   83 ALPH1=ALPH*0.5
```

```
      M=1
      NN=0 $ IO=0
      DO 1 K=KI, KKF
      DX(K)=XH(K+1)-XH(K)
    1 H(K,M)=HO1+C5*0.5*(XH(K)**2)
      H(KF,M)=HO1
      AP=1.0-(1.0/EXP(ALPH))
      DO 5 K=KI, KF
      APC=AP*((HO1/H(K,M))**2)
      APO=1.0-APC
    5 P(K,M)=-(1.0/ALPH)*ALOG(APO)
      WRITE(6,668) (K, P(K,M), K=KI, KF)
      DO 8 K=KI, KF
    8 PS(K)=P(K,M)
      HO(M)=HO1
      T(M)=1.0
      HE=HO(M)
      IS=2
      CALL DVD
      CALL HDT
      PAI(KF)=0.0
      DO 6 K=KI, KKF
      J=KF-K
    6 PAI(J)=PAI(J+1)-DX(J)*(DEN(J,M)+DEN(J+1,M))*0.5
      DO 4 K=KI, KF
    4 VD(K)=(PAI(K)*B(K))/(H(K,M)**3*DEN(K,M))
      CALL INTEG1(XH(KI),XH(KF),2,VD,KF,VALUE,IER)
      EBF=VALUE-ALPH/(16.0*(H(KI,M)*PHZ)**2)
      EF1=EBF
      DO 181 K=KA, KF
      DO 181 J=KA, KF
      BET(K,J)=0.0
  181 CONTINUE
      GO TO 499
   56 M=2 $ GO TO 58
   57 M=3
   58 NN=0 $ IO=0
      IF(MM.LE.4)580,581
  580 HO(M)=HO(M-1)-20.0E-6
      GO TO 983
  581 BM=MM $ BMF=MF
      IF(MM.LE.15) 982,988
  982 RA1=RA*(1.0-BM/BMF)
      HO(M)=(1.0-RA1)*HO(M-1)
      GO TO 983
  988 HO(M)=(1.0-0.15)*HO(M-1)
  983 DT(M)=HO(M-1)-HO(M)
   23 T(M)=T(M-1)+DT(M)
      IF(MM.EQ.2) GO TO 161
C     CALCULATION OF THE INITIAL GUESSED PRESSURE BY LINEAR
C     EXTRAPOLATION.
      T1=(T(M)-T(M-1))/(T(M-2)-T(M-1))
      T2=(T(M)-T(M-2))/(T(M-1)-T(M-2))
      DO 751 K=KI, KF
  751 P(K,M)=T1*P(K,M-2)+T2*P(K,M-1)
      IS=2 $ II=2 $ CALL DVD $ CALL HDT
      IS=3 $ CALL INTEG
      HE1=HO(M-1)
```

```
      HE=HO(M)
      GO TO 164
  161 DO 162 K=KI, KF
  162 P(K,M)=P(K,M-1)
      KC=4 $ WRITE(6,200) KC
      IS=2 $ II=2$ CALL DVD $ CALL HDT
  164 EF1=EBF
  499 IF(NN+1.EQ.1) 1613, 118
 1613 DO 1614 K=KI, KKF
 1614 PS(K)=P(K,M)
C     CALCULATION OF THE SYSTEM EQUATIONS AND THE DERIVATIVES
C     OF THE SYSTEM EQUATIONS.
  118 IS=3 $ II=3 $ CALL DVD
      PKA=P(KA,M)
      C8=EBF/(4.0*A(KF))
      DO 71 K=KA, KKF
      KK=K-KA+1
      C8DXP=C8/DX(K)*(P(K+1,M)-P(K,M))*DEN(K,M)/VIS(K)*(H(K+1,M)
     X+H(K,M))**2
      EE(KK)=C8DXP*(H(K+1,M)+H(K,M))-(PAI(K+1)+PAI(K))
      DO 71 J=KA, KKF
      JJ=J-KA+1
      IF(J.EQ.KA) 72,  78
   72 QQQ=0.0
      DO 73 I=KI, KA
   73 QQQ=QQQ+(Q(K,I)+Q(K+1,I))*P(I,M)
      QQQ=QQQ/P(KA,M)
      GO TO 74
   78 QQQ=Q(K,J)+Q(K+1,J)
   74 R(KK,JJ)=-3.0*C6*C8DXP*QQQ-(BET(K+1,J)+BET(K,J))
      IF(J.EQ.K) GO TO 75
      IF(J.EQ.K+1) GO TO 76
      GO TO 71
   75 SIGN=-1.0
      GO TO 77
   76 SIGN=1.0
   77 R(KK,JJ)=R(KK,JJ)+(C8/(DX(K)*VIS(K)))*((P(K+1,M)-P(K,M))*(DEND
     X(K,M)-DEN(K,M)*VISD(K)/VIS(K))+SIGN*DEN(K,M))*((H(K+1,M)+
     XH(K,M))**3)
   71 CONTINUE
      IE=KKF-KA+1
  467 IG=KF-KA
C     LIBRARY SUBROUTINE, IN1SP, IS THE OPERATION OF MATRIX
     INVERSION WHERE THE GAUSSIAN ELIMINATION METHOD IS USED.
      CALL IN1SP(R,IG,1.E-7,IEER,51,TEM,NI)
      IF(IEER) 1503 , 1503, 1504
 1504 WRITE(6,200) IEER
      GO TO 1006
 1503 DO 100 KK=KI,IE
      AS=0.0
      DO 101 JJ=KI, IE
  101 AS=AS+R(KK,JJ)*EE(JJ)
      K=KK+KA-1
      DP(K)=-AS
      P(K,M)=P(K,M)+DP(K)
      PS(K)=P(K,M)
  100 CONTINUE
      WRITE(6,200) NN, IC
```

```
      WRITE(6,217) EF1, EDF
      WRITE(6,842) (K,EE(K),K=KI,IE)
      WRITE(6,843) (K,DP(K),K=KA,KKF)
      DO 146 K=KA, KKF
      SU=1.0-DP(K)
      IF(SU) 995, 995, 146
  995 WRITE(6,217) SU $ GO TO 1000
  146 CONTINUE
  133 PW=0.0 $ PQ=0.0
      DO 106 K=KA, KKF
      PW=PW+DP(K)
  106 PQ=PQ+P(K,M)
      P-U=ABS(PW/PQ)
      KA1=KA-1
  115 IF(PRO-0.0002) 108, 108, 117
  117 NN=NN+1 $ IF(NN.LE.20) 111, 192
  111 IF(M.EQ.1) 112, 113
  112 IO=2 $ II=1 $ CALL DVD $ CALL HDT
      PAI(KF)=0.0
      DO 791 K=KI, KKF
      J=KF-K
  791 PAI(J)=PAI(J+1)-DX(J)*(DEN(J,M)+DEN(J+1,M))*0.5
      CALL INTEG
      GO TO 158
  113 IO=2$ II=1 $ CALL DVD
  981 CALL HDT
      IO=3 $ KO=3 $ CALL INTEG
      GO TO 158
  158 IF(IO+1.EQ.1) 116, 152
  152 IF(NN+1.EQ.1) 153, 118
  108 PW=0.0 $ PQ=0.0
      NN=0
      DO 224 K=KKI,KKF
      PW=PW+P(K,M)-PS(K)
  224 PQ=PQ+P(K,M)
      PRQ=ABS(PW/PQ)
C     THE CALCULATION OF THE INTERGRATED INLET PRESSURE.
      DO 322 K=KI, KA
  322 VO(K)=PAI(K)/(H(K,4)**3*DEN(K,M))
      QKA=1.0-1.0/EXP(ALPH*P(KA,M))
      A(KI)=0.0 $ KA1=KA-1
      DO 323 K=KI, KA1
      IT=K $ ITI=K+1
      CALL INTEG2(XM(IT),XM(ITI),1,VO,KF,VALUE,IER)
  323 A(ITI)=A(IT)+VALUE
      DO 324 K=KI, KA1
      QK=QKA*A(K)/A(KA)
      QK=1.0-QK
      IF(QK)351, 351, 324
  324 P(K,M)=-ALOG(1.0-QK)/ALPH
      GO TO 358
  351 KA1=KA-1 $ WRITE(6,217) QK
      DO 330 K=KI, KA1
  330 P(K,M)=PS(K)*P(KA,M)/PKA
  358 WRITE(6,844) (K,P(K,M),K=KI,KA)
  360 DO 360 K=KI, KKF
  360 PS(K)=P(K,M)
      IF(M.EQ.12) 471, 427
```

```
  427 IF(PRQ.LE.0.0002) 197, 227
  471 IF(PRQ.LE.0.001) 197, 227
  227 IO=IO+1 $ IF(IO.LE.30) 111, 192
  153 EBF=0.5*(CC(KF)-ALPH/(16.0*(H(KI,M)*PHZ)**2)+EF1)
      EF1=CC(KF)-ALPH/(16.0*(H(KI,M)*PHZ)**2)
      GO TO 118
  192 NG=1
  197 DO 198 K=KI, KKF
      SP=ABS(P(K,M))
      IF(SP-1.0) 198, 198, 1000
  198 CONTINUE
C     THIS CALL IS FOR THE CALCULATION OF LOAD BY THE SUBROUTINE
C     INTEG1.
      CALL INTEG2(XH(KI),XH(KF),2,P(1,M),KF,VALUE,IER)
      W(M)=2.0*VALUE
      IF(MM.GE.7) 851, 852
  851 PUNCH 205, (P(K,M), K=KI, KF)
      PUNCH 231, H(KA,M), T(M)
      WRITE(6,668) (K, PAI(K), K=KI, KKF)
C     PRINT OUT-LOAD, CENTER FILM THICKNESS, PRESSURE,
  852 AUT=ALPH*0.25/(H(KI,M)**2)
      V(M)=-AP/(C4*EBF)
      WRITE(6,1009) AUT
      VC=AP*(HO(M)**2)*PHO/ALPH
      WRITE(6,1009) VC
      DO 853 K=KI,KF
  853 VD(K)=XH(K)/H(K,M)**3
      DP(KI)=0.0
      DO 854 K=KI,KKF
  854 DP(K+1)=DP(K)+0.5*(VD(K+1)+VD(K))*DX(K)
      VF=-AP/(C4*(DP(K)*ALPH-ALPH/(16.0*(H(KI,M)*PHZ)**2)))
      WRITE(6,217) VF,DP(KF)
      WRITE(6,220) MM,W(M),HO(M),T(M),DT(M),V(M)
      WRITE(6,210) (K, P(K,M), K=KKI, KF)
      WRITE(6,211) (K, H(K,M), K=KI, KF)
      WRITE(6,215) (K, D(K,M), K=KI, KF)
      IF(MM.LE.2) GO TO 863
      DO 861 K=KI, KF
  861 VD(K)=V(M)*(OMEG1(M)*D(K,M)+OMEG2(M)*D(K,M-1)+OMEG3(M)*D(K,M-2)
     X-1.0)
      WRITE(6,209) (K, VD(K), K=KI, KF)
  863 WS=4.0*((PH/E)**2)*W(M)
      WT=1.5*W(M)
      WRITE(6,217) WT, WS
      IS=2 $ II=2$ CALL DVD $ CALL HDT
  557 IF(MM-2) 50, 50, 52
   52 DO 41 M=1,2
      T(M)=T(M+1)
      HO(M)=HO(M+1)
      DO 41 K=KI, KF
      DEN(K,M)=DEN(K,M+1)
      D(K,M)=D(K,M+1)
      H(K,M)=H(K,M+1)
      P(K,M)=P(K,M+1)
   41 CONTINUE
      IF(HO(M).LE.10.0E-6) 1000,1099
 1099 IF(MM.EQ.3) 517, 518
  517 W3=W(M) $ H3=HO(M) $ T3=T(M) $ V3=V(M) $ DT3=DT(M) $ GO TO 50
```

```
  510 W(MM)=W(M) $ T(MM)=T(M) $ HO(MM)=HO(M) $ V(MM)=V(M) $ DT(MM)=DT(M)
   50 CONTINUE
1000 WRITE(6,829)
1000 KM=MM
     DO 583 I=KI,KM
     IF(I.EQ.3) 519, 583
  519 W(I)=W3$H(I)=H3$T(I)=T3$V(I)=V3$DT(I)=DT3
  583 WRITE(6,221) I, W(I),HO(I),T(I),DT(I),V(I)
     STOP 1
  200 FORMAT(4I5, 2F10.3, F10.1, F10.0)
  201 FORMAT(4F15.8)
  202 FORMAT(5E15.2)
  203 FORMAT(F15.2, F15.2, E15.2, F15.3)
  204 FORMAT(2F10.1, E10.2, F10.1)
  205 FORMAT(6E12.5)
  206 FORMAT(6E12.5)
  207 FORMAT(8F10.1)
  209 FORMAT(5X//40X,*RELATIVE VELOCITY, V(K,M)=*//2X,*K*,20X,*K*  ,20X,
     X *K*,20X,*K*,20X,*K*,20X,*K*//(6(I3,E15.7,3X)))
  210 FORMAT(3X//50X, *P(K,M)=*//2X, *K*, 20X, *K*, 20X, *K*,
     X20X, *K*, 20X, *K*,20X, *K*//(6(I3, E15.7, 3X)))
  211 FORMAT(3X//50X, *H(K,M)=*//2X, *K*, 20X, *K*, 20X, *K*,
     X20X, *K*, 20X, *K*,20X, *K*//(6(I3, E15.7, 3X)))
  215 FORMAT(3X//50X, *D(K,M)=*//2X, *K*, 20X, *K*, 20X, *K*,
     X20X, *K*, 20X, *K*,20X, *K*//(6(I3, E15.7, 3X)))
  212 FORMAT(3X//15X, *THE RIGID BODY PRESSURE, P(K,M)=*//2X,
     X*K*, 20X, *K*, 20X, *K*, 20X, *K*,20X, *K*, 20X, *K*//(6(I3,
     XE15.7, 3X)))
  223 FORMAT(1H1, 3X, *M=*, I3, 5X, *W(M)=*, E15.7, 4X, *WO=*,
     XE15.7, 5X, *HO(M)=*, E15.7, 5X, *V=*, E15=7)
  220 FORMAT(1H1, 3X, *M=*, I3, 3X, *W(M)=*, E15.7, 3X, *HO(M)=*,
     XE15.7, 3X, *T(M)=*, E15.7, 3X, *DT(M)=*, 515.7,2X, *V(M)=*,E15.7)
  221 FORMAT(3X,*M=*,I3,3X,*W(M)=*,E15.7,3X,*HO(M)=*,
     XE15.7,3X,*T(M)=*,E15.7,3X,*DT(M)=*,E15.7,2X,*V(M)=*,E15.7)
  600 FORMAT(5X///5I5, 5X, *EP IS TOO SMALL*)
  231 FORMAT(2E20.10)
  640 FORMAT(3X, *N-R, PRESSURE DATA*///(6(I5, F10.8))////)
  703 FORMAT(5X, I5//(4(I5, F14.6)))
  710 FORMAT(3X, I5, 4F12.6)
  731 FORMAT(1H1, 3X, *M=*, I3, 5X, *W(M)=*, E13.7, 5X, *WO=*, E13.7,
     X5X, *HO(M)=*, E13.7)
  666 FORMAT(2I5, 7E16.8)
  669 FORMAT(1H1//(6(I4, 1X, E16.8)))
  668 FORMAT(2X//(6(I4, 1X, E16.8)))
  603 FORMAT(5X//50X, *MATRIX K(K,J)=*//(6(2I4,E12.5)))
 1008 FORMAT(1H1/2X, *V=*, E16.8)
 1009 FORMAT(2X, *V1=*, E16.8)
 1600 FORMAT(45X, *W(M)=*, E16.8)
 1010 FORMAT(45X, *TRUE V=*, E15.8)
  210 FORMAT(5(F11.8, F14.8))
  217 FORMAT(5E15.7)
  829 FORMAT(2X, *MATRIX IS SINGULAR*, 2X)
  844 FORMAT(40X,*P(K,M)=*//(6(I4,2X,E15.7)))
  841 FORMAT(50X,*XM(K)=*//(6(I4,2X,E15.5)))
  842 FORMAT(40X,*EL(K)=*//(6(I4,2X,E15.7)))
  843 FORMAT(40X,*DP(K)=*//(6(I4,2X,E15.7)))
     END
     SUBROUTINE HDT
```

```
C       CALCULATION OF FILM THICKNESS AND COEFFICIENTS OF LAGRANGIAN
C       THREE-POINT QUADRATURE.
        COMMON/A/KF, ALPH, EN, ED, HE, HE1, ALPH1, MM
        COMMON KI, KA, KKI, KKF, KF2, KF3, V, KKE, IS, N, NN, PO, K, M,
       1PM, PC, KO, EP, EO, W, WW, AM, RA, RO, PNR, PDI, XH, DX, DI, D,
       2HG,H,P,VIS,VISD,DEN,DEND,T,DT,VD,DP,HO,SE,A,B,C,SD,AM,PS,
       3OMEG3,OMEG2,OMEG1,DENT,DD,DS,C4,C5,II,Q,PAI,BET,P1,P2,VIS1,
       4VIS2,VIS3,DPV,C6,EDF,SUBV,CC,EE,PRA,DPR,R
        DIMENSION XH(51),DX(51),D(51,3),HG(51,3),H(51,3),DI(51),
       1P(51,3),VIS(51),VISD(51),DEN(51,3),DEND(51,3),T(35),V(35),
       2DT(35),VD(51),DP(51),HO(50),W(35),SE(51),A(51),B(51),CC(51),
       3F(51),R(51,51),BET(51,51),SD(51),PS(51),OMEG3(3),OMEG2(3),
       4OMEG1(3),DENT(51),Q(51,51),PAI(51),SUBV(51),C(2,3,51),EE(51)
        DO 300 K=KI, KF
        DS=0.0
        DO 301 J=KI, KF
  301   DS=Q(K,J)*P(J,M)+DS
  300   D(K,M)=-C6*DS
        DO 303 K=KI, KF
        IF(KF3.EQ.1) 22, 42
   42   IF(MM.EQ.1) 21, 22
   21   HG(K,M)=HO(M)+0.5*C5*(XH(K)**2)
        H(K,M)=HG(K,M)+D(K,M)
        GO TO 303
   22   HG(K,M)=HO(M)+0.5*C5*(XH(K)**2)
        H(K,M)=HG(K,M)+D(K,M)
  303   CONTINUE
        HO(M)=H(KF,M)
  341   IF(MM-1) 310, 310, 311
  311   DT(M)=HO(M-1)-HO(M)
        T(M)=T(M-1)+DT(M)
        IF(MM-2) 310, 335, 331
  335   OMEG1(M)=1.0/DT(M)
        GO TO 310
  331   OMEG3(M)=(T(M)-T(M-1))/((T(M-2)-T(M-1))*(T(M-2)-T(M)))
        OMEG2(M)=(T(M)-T(M-2))/((T(M-1)-T(M-2))*(T(M-1)-T(M)))
        OMEG1(M)=((T(M)-T(M-1))+(T(M)-T(M-2)))/((T(M)-T(M-1))*(T(M)-T(M-2)
       X))
  310   CONTINUE
        RETURN
        END
        SUBROUTINE INTEG
C       CALCULATION OF THE INTEGRAL AND DERIVATIVE OF THE INTEGRAL
C       IN WHICH THE INTEGRAND IS TIME DERIVATIVE OF THE
C       PRODUCT OF DENSITY AND FILM THICKNESS.
        COMMON/A/KF, ALPH, EN, ED, HE, HE1, ALPH1, MM
        COMMON KI, KA, KKI, KKF, KF2, KF3, V, KKE, IS, N, NN, PO, K, M,
       1PM, PC, KO, EP, EO, W, WW, AM, RA, RO, PNR, PDI, XH, DX, DI, D,
       2HG,H,P,VIS,VISD,DEN,DEND,T,DT,VD,DP,HO,SE,A,B,C,SD,AM,PS,
       3OMEG3,OMEG2,OMEG1,DENT,DD,DS,C4,C5,II,Q,PAI,BET,P1,P2,VIS1,
       4VIS2,VIS3,DPV,C6,EDF,SUBV,CC,EE,PRA,DPR,R
        DIMENSION XH(51),DX(51),D(51,3),HG(51,3),H(51,3),DI(51),
       1P(51,3),VIS(51),VISD(51),DEN(51,3),DEND(51,3),T(35),V(35),
       2DT(35),VD(51),DP(51),HO(50),W(35),SE(51),A(51),B(51),CC(51),
       3F(51),R(51,51),BET(51,51),SD(51),PS(51),OMEG3(3),OMEG2(3),
       4OMEG1(3),DENT(51),Q(51,51),PAI(51),SUBV(51),C(2,3,51),EE(51)
        KA1=KA-1
    55  IF(MM-2) 3,1, 2
```

```
    1 DO 5 K=KI, KF
      DENT(K)=(DEN(K,M)-DEN(K,M-1))/DT(M)
      SD(K)=(D(K,M)-D(KA,M)-D(K,M-1)+D(KA,M-1))/DI(M)
    5 SE(K)=DEN(K,M)*(SD(K)-1.0)+H(K,M)*DENT(K)
      PAI(KF)=0.0
      DO 4 K=KI, KKF
      J=KF-K
    4 PAI(J)=PAI(J+1)+DX(J)*(SE(J)+SE(J+1))*0.5
      GO TO 31
    2 DO 10 K=KI, KF
      DENT(K)=OMEG3(M)*DEN(K,M-2)+OMEG2(M)*DEN(K,M-1)+
     XOMEG1(M)*DEN(K,M)
      SD(K)=OMEG3(M)*DEN(K,M-2)*D(K,M-2)+OMEG2(M)*DEN(K,M-1)*D(K,M-1)
     X+OMEG1(M)*DER(K,M)*D(K,M)
   10 SE(K)=-DEN(K,M)+SD(K)*HG(K,M)*DENT(K)
      PAI(KF)=0.0
      DO 25 K=KI, KKF
      J=KF-K
   25 PAI(J)=PAI(J+1)+DX(J)*(SE(J)+SE(J+1))*0.5
   31 IF(IS.EQ.3) 15, 20
   15 DO 16 K=KA1, KF
      BET(KF,K)=0.0
   16 CONTINUE
      KA1=KA-1
      KF2=KF-2
      DO 150 K=KA, KF
      DO 100 J=KA, KF
      R(K,J)=0.0  ! IF(J.EQ.KA) 151, 152
  151 DO 153 I=KI, KA
  153 R(K,J)=R(K,J)+Q(K,I)*P(I,M)/P(KA,M)
      GO TO 100
  152 R(K,J)=Q(K,J)
  150 CONTINUE
      DO 101 K=KA, KF
      DO 101 J=KA, KF
      SSS=0.0
      DO 103 N=K, KKF
  103 SSS=SSS-DEN(N,M)*R(N,J)*(XH(N+1)-XH(N-1))
      SS=SSS+DEN(K,M)*R(K,J)*DX(K-1)
      SS=SS-DEN(KF,M)*R(KF,J)*DX(KKF)
      BET(K,J)=OMEG1(M)*C6*SS*0.5
      IF(J-K) 101, 107, 108
  107 BET(K,J)=BET(K,J)+DEND(J,M)*DX(J)*(OMEG1(M)*H(J,M)-1.0)*0.5
      GO TO 101
  108 BET(K,J)=BET(K,J)+DEND(J,M)*(XH(J+1)-XH(J-1))*(OMEG1(M)
     X*H(J,M)-1.0)*0.5
  101 CONTINUE
      DO 33 K=KA1, KF
   33 BET(KF,K)=0.0
      GO TO 60
    3 DO 43 K=KA, KF
      DO 43 J=KA, KF
      BET(K,J)=0.0
   43 CONTINUE
   60 DO 47 K=KI, KF
   47 VG(K)=B(K)*PAI(K)/(-H(K,1)**3*DEN(K,M))
      CALL INTEG2(XH(KI),XH(KF),Z,VG, KF, VALUE, IER)
      CC(KF)=VALUE
```

```
   20 CONTINUE
      RETURN
      END
      SUBROUTINE DVD
C     CALCULATION OF DENSITY, VISCOSITY AND THEIR DERIVATIVES
C     WITH RESPECT TO PRESSURE.
      COMMON/A/KF, ALPH, EA, ED, NL, NL1, ALPH1, MM
      COMMON KI, KA, KKI, KKF, KF2, KF3, V, KKE, IS, N, NN, PO, K, M,
     1PM, PC, K3, EP, EO, W, WW, MM, KA, KO, PNR, PDI, XH, DX, DI, D,
     2HO,H,P,VIS,VISD,DEN,DEND,T,DT,VO,DP,HO,SE,A,B,C,SD,AM,PS,
     3OMEG3,OMEG2,OMEG1,DEN1,DD,DS,C4,C5,II,W,PAI,BET,P1,P2,VIS1,
     4VIS2,VIS3,DPV,C6,EBF,SUBV,CC,EE,PKA,DPR,R
      DIMENSION XH(51),DX(51),D(51,3),HO(51,3),H(51,3),DI(51),
     1P(51,3),VIS(51),VISD(51),DEN(51,3),DEND(51,3),T(35),V(35),
     2DT(35),VO(51),DP(51),HO(50),W(35),SE(51),A(51),B(51),CC(51),
     3F(51),R(51,51),BET(51,51),SD(51),PS(51),OMEG3(3),OMEG2(3),
     4OMEG1(3),DEN1(51),W(51,51),PAI(51),SUBV(51),C(2,3,51),EE(51)
      IF(IS-2) 200, 202, 207
  200 VIS(K)=EXP(ALPH*P(K,M))
      VISD(K)=ALPH*VIS(K)
      DEN(K,M)=1.0+(EN*P(K,M))/(1.0+ED*P(K,M))
      DEND(K,M)=EN/((1.0+P(K,M)*ED)**2)
      GO TO 20
  202 DO 205 K=KI, KF
      VIS(K)=EXP(ALPH*P(K,M))
      VISD(K)=ALPH*VIS(K)
      DEN(K,M)=1.0+(EN*P(K,M))/(1.0+ED*P(K,M))
  205 DEND(K,M)=EN/((1.0+P(K,M)*ED)**2)
      GO TO 206
  207 DO 209 K=KA, KKF
      P3=(P(K+1,M)+P(K,M))/2.0
      VIS(K)=EXP(ALPH*P3)
      VISD(K)=0.5*ALPH*VIS(K)
      DEN(K,M)=1.0+(EN*P3)/(1.0+ED*P3)
  209 DEND(K,M)=0.5*EN/((1.0+P3*ED)**2)
  206 IF(II.EQ.1) 46, 20
   46 KA1=KA-1
      IF(NN+1.EQ.1) 20, 88
   88 DO 47 K=KI, KA1
   47 P(K,M)=P(K,M)**P(KA,M)/PKA
   20 CONTINUE
      RETURN
      END
      SUBROUTINE INTEG1(G1,G2,KCT,F,NP,VALUE,IERR )
*     INTEGRATES THE NON EQUIDISTANTLY TABULATED FUNCTION F(X(I))
*     BETWEEN THE LIMITS A AND B.
*     A MODIFIED METHOD OF OVERLAPPING PARABOLAS IS EMPLOYED.
*     A SECOND ENTRY POINT 'INTEG2' IS PROVIDED FOR MORE THAN ONE
*     INTEGRATION ON THE SAME DIVISIONS OF X.  THIS SAVES THE TIME
*     OF CALCULATING THE WEIGHTING FUNCTIONS.
*     ARGUMENTS -
*     A          LOWER LIMIT OF INTEGRATION.
*     B          UPPER LIMIT OF INTEGRATION.
*     X          ARRAY OF ARGUMENT VALUES.  MUST BE MONOTONICALLY
*                INCREASING AND MUST BE DIMENSIONED NP.
*     F          ARRAY OF FUNCTION VALUES.  MUST BE DIMENSIONED NP.
*     NP         NUMBER OF POINTS.  NP MUST BE GREATER THAN 3.
*     VALUE      RESULTANT VALUE OF THE INTEGRATION.
```

```
*       C          WEIGHTING FUNCTION PASSED TO THE MAIN PROGRAM
*                  FOR STORAGE.
*       IERR       RESULTANT ERROR PARAMETER.
*       REQUIRED SUBPROGRAMS - NONE
*       COMMON STORAGE -
*       THE WEIGHTING FUNCTION C IS STORED IN THE MAIN PROGRAM AND
*       REQUIRES THE FOLLOWING DIMENSION STATEMENT WHERE D.GE.NP.
*       ERROR INDICATIONS -
*       IERR = 0   INDICATES NO ERROR.
*       IERR = 1   INDICATES NP IS LESS THAN 4.
*       IERR = 2   INDICATES THE LIMITS OF INTEGRATION ARE OUT OF
*                  THE RANGE OF THE TABLE.
        COMMON/A/KF, ALPH, EN, ED, HE, HE1, ALPH1, MM
        COMMON KI, KA, KKI, KKF, KF2, KF3, V, KKE, IS, N, NN, PO, K, M,
       1PM, PC, KS, EP, EU, W, WW, WM, RA, KO, PNR, PDI, XH, DX, DI, D,
       2HG,H,P,VIS,VISD,DEN,DEND,T,DT,VD,DP,HO,SE,A,B,C,SD,AM,PS,
       3OMEG3,OMEG2,OMEG1,DENT,DU,DS,C4,C5,II,Q,PAI,BET,P1,P2,VIS1,
       4VIS2,VIS3,DPV,C6,EBF,SUBV,CC,EE,PKA,DPR,R
        DIMENSION XH(51),DX(51),D(51,3),HG(51,3),H(51,3),DI(51),-
       1P(51,3),VIS(51),VISD(51),DEN(51,3),DEND(51,3),T(35),V(35),
       2DT(35),VD(51),DP(51),HO(50),W(35),SE(51),A(51),B(51),CC(51),
       3F(51),R(51,51),BET(51,51),SD(51),PS(51),OMEG3(3),OMEG2(3),
       4OMEG1(3),DENT(51),Q(51,51),PAI(51),SUBV(51),C(2,3,51),EE(51)
*       NP MUST BE GREATER THAN 3
        IF (NP.LE.3) GO TO 96
*       CALCULATION OF INTERVALS OF X
        NH=NP-1
        DO 10 I=1,NH
   10   DX(I)=XH(I+1)-XH(I)
        DO 20 I=1, NH
*       DEFINE COEFFICIENTS OF FIRST PARABOLA
        IF(I.EQ.1) GO TO 15
        C(1,1,I)=-DX(I)**3/(6.0*DX(I-1)*(DX(I-1)+DX(I)))
        C(1,2,I)=DX(I)*(3.0*DX(I-1)+DX(I))/(6.0*DX(I-1))
        C(1,3,I)=DX(I)*(3.0*DX(I-1)+2.0*DX(I))/(6.0*(DX(I-1)+DX(I)))
   15   CONTINUE
        IF(I.EQ.NH) GO TO 20
*       DEFINE COEFFICIENTS OF SECOND PARABOLA
        C(2,1,I)=DX(I)*(2.0*DX(I)+3.0*DX(I+1))/(6.0*(DX(I)+DX(I+1)))
        C(2,2,I)=DX(I)*(DX(I)+3.0*DX(I+1))/(6.0*DX(I+1))
        C(2,3,I)=-DX(I)**3/(6.0*DX(I+1)*(DX(I)+DX(I+1)))
   20   CONTINUE
        ENTRY INTEG2
*       INITIALIZE SUMMATION VARIABLE
        VALUE=0.0
        IF(G2-G1) 40,92,30
*       B IS GREATER THAN A
   30   ALIM=G1
        BLIM=G2
        SIGN = 1.0
        GO TO 50
*       A IS GREATER THAN B
   40   ALIM=G2
        BLIM=G1
        SIGN =-1.0
   50   NH=NP-1
        IF(KCT.EQ.1) 125, 123
*       CALCULATION OF INTEGRAL OVER SUBINTERVAL
```

```
  123 DO 80 I=1, NH
      SUBV(I)=0.0
      IF(XH(I).EQ.ALIM) SUBV(I)=C(2,1,I)*F(I)+C(2,2,I)*F(I+1)
     X+C(2,3,I)*F(I+2)
      IF(XH(I+1).EQ.BLIM) SUBV(I)=C(1,1,I)*F(I-1)+C(1,2,I)*F(I)
     X+C(1,3,I)*F(I+1)
      IF(XH(I).GT.ALIM.AND.XH(I+1).LT.BLIM) SUBV(I)=0.5*(C(1,1,I)
     X*F(I-1)+(C(1,2,I)+C(2,1,I))*F(I)+(C(1,3,I)+C(2,2,I))*F(I+1)+
     XC(2,3,I)*F(I+2))
   80 VALUE=VALUE+SUBV(I)
      VALUE=SIGN*VALUE
      GO TO 92
  125 DO 110 I=1, NH
      SUBV(I)=0.0
      IF(XH(I).EQ.ALIM) 111, 110
  111 IF(I.EQ.NH) 113, 114
  113 SUBV(I)=C(1,1,I)*F(I-1)+C(1,2,I)*F(I)+C(1,3,I)*F(I+1)
      GO TO 120
  114 IF(I.GE.2) 115, 116
  115 SUBV(I)=0.5*(C(1,1,I)*F(I-1)+(C(1,2,I)+C(2,1,I))*F(I)+(C(1,3,I)
     X+C(2,2,I))*F(I+1)+C(2,3,I)*F(I+2))
      GO TO 120
  116 SUBV(I)=C(2,1,I)*F(I)+C(2,2,I)*F(I+1)+C(2,3,I)*F(I+2)
  120 VALUE=SIGN*SUBV(I) $ GO TO 92
  110 CONTINUE
*     SET ERROR PARAMETER FOR NORMAL RETURN
   92 IERR = 0
      RETURN
*     SET ERROR PARAMETER FOR TOO FEW POINTS
   96 IERR = 1
      RETURN
*     SET ERROR PARAMETER FOR A AND/OR B OUT OF RANGE OF TABLE
   97 IERR = 2
      RETURN
      END
*  END OF RECORD
```

LIST OF SYMBOLS

a	Half of Hertzian width
a_1	coefficient of density
$A_1 = \frac{a}{P_o}$	
b	coefficient of density
$B = \frac{b}{P_o}$	
c	constant in deformation formula
c_1	constant in deformation formula of cylinder 1
c_2	constant in deformation formula of cylinder 2
c_3	coefficient of deformation formula
d	Deformation
$D = \frac{d}{R}$	
E	Equivalent Young's modulus
E_1	Young's modulus of cylinder 1
E_2	Young's modulus of cylinder 2
h	Film thickness
$H = \frac{h}{R}$	
h'_o	Rigid center film thickness
h_o	center film thickness
$H_o = \frac{h_o}{R}$	
h_g	geometrical film thickness

$H_g = \frac{h_o}{R}$	
h_m	Minimum film thickness
$H_m = \frac{h_m}{R}$	
i	A dummy index
$I_{K,m}$	See Eq. (B.7)
j	A dummy index
k	A dummy index
$K_j(-X_K, -Z_j)$	See Eqs. (42), (43) and (44)
$L(-X_K, -Z_j)$	See Eq. (62)
m	An index for time step
N/m^2	Newton/meter^2
P	Pressure
P_o	Center pressure
$P = \frac{P}{P_o}$	
$P_{HZ} = \frac{P_o}{E}$	Hertzian pressure
R	Radius of equivalent cylinder
R_1	Radius of cylinder 1
R_2	Radius of cylinder 2
$RR_{K,j}$	See Eq. (B.10)
t	time
$T = \frac{v_o}{R}t$	

$$S_j = \frac{u_j^2}{2}(\ell n |u_j| - \frac{3}{2})$$

$$u_j = -Z_j - X_K$$

v Approach velocity

$$V = \frac{12\mu_s}{ER}$$

v_o center approach velocity

$$V_{o,m} = \frac{12\mu_s}{ER}$$

v_d Deformation velocity

x coordinate along film

$$X = \frac{x}{a}$$

X_{KA} Coordinate separating the inlet and middle region

$$X_{KA} = \frac{X_{KA}}{a}$$

w Load per unit width of cylinder

$$\bar{W} = \frac{w}{ER}$$

ξ Dummy coordinate along film

$$Z = \frac{\xi}{a}$$

α Pressure-viscosity coefficient

$$\bar{\alpha} = \frac{\alpha}{P_o}$$

β Second pressure-viscosity coefficient

$$\bar{\beta} = \frac{\beta}{P_o}$$

$\gamma_m(-X_K)$	See Eq. (60)
μ	viscosity
μ_s	Ambient viscosity
$\bar{\mu} = \frac{\mu}{\mu s}$	
ν_1	Poisson's ratio of cylinder 1
ν_2	Poisson's ratio of cylinder 2
ω_j	See Eqs. (56), (57) and (58)
$\Psi_m(P)$	System equation
$\Delta \cdot \Psi_m(p)$	Derivative of $\Psi_m(p)$ with respect to p_m
ρ	Density
ρ_s	Ambient density
$\bar{\rho} = \frac{\rho}{\rho_s}$	

BIBLIOGRAPHY

1. D. Dowson and G. R. Higginson, "The Effect of Material Properties on the Lubrication of Elastic Rollers", Journal of Mechanical Engineering Science, Vol. 2, No. 3, p. 188.

2. H. S. Cheng and B. Sternlicht, "A Numerical Solution for the Pressure, Temperature, Film Thickness Between Two Infinitely Long Lubricated Rolling and Sliding Cylinders, Under Heavy Loads", ASME Transaction, Journal of Basic Engineering, Vol. 87, 1965, pp. 695-707.

3. H. S. Cheng, "A Refined Solution to the Thermal-Elastohydrodynamic Lubrication of Rolling and Sliding Cylinders", Transactions of the American Society of Lubrication Engineers, Vol. 8, 1965, pp. 397-410.

4. H. Christensen, "The Oil Film in a Closing Gas", Proceedings of the Royal Society, London, Vol. 266, Series A, 1961, pp. 312-328.

5. K. Herrebrugh, "Elastohydrodynamic Squeeze Films Between Two Cylinders in Normal Approach", ASME Transaction, Journal of Lubrication Technology, April, 1970, pp. 292-302.

6. F. P. Bowden and D. Tabor, "The Friction and Lubrication of Solids, Part I", Oxford University Press.

7. C. W. Allen, D. P. Townsend and E. V. Zaretsky, "Elastohydrodynamic Lubrication of a Spinning Ball in a Nonconforming Groove", ASME Transaction, Journal of Lubrication Technology, January, 1970, pp. 89-96.

8. "Viscosity and Density of Over 40 Lubricating Fluids of Known Composition at Pressures to 150,000 psi and Temperatures to 425^{o}F", A Report of the American Society of Mechanical Engineers Research Committee on Lubrication, American Society of Mechanical Engineers, New York, Vol. II, 1953, Appendix VI.

9. D. Dowson and A. V. Whitaker, "A Numerical Procedure for the Solution of Elastohydrodynamic Problem of Rolling and Sliding Contacts Lubricated by Newtonian Fluid", Proceedings of the Institute of Mechanical Engineers, Vol. 180, Part 3, Series B, 1965, pp. 57-71.

10. M. A. Plint, "Traction in Elastohydrodynamic Contacts", Proceedings of the Institute of Mechanical Engineers, Part 1, Vol. 182, 1967-68, pp. 300-306.

11. K. L. Johnson and R. Cameron, "Shear Behavior of Elastohydrodynamic Oil Film at High Rolling Contact Pressures", Proceedings of the Institute of Mechanical Engineers, 1967-68, Vol. 182, p. 307.

12. D. Dowson and T. L. Wholmes, "Effect of Surface Quality upon the Traction Characteristics of Lubricated Cylindrical Contacts", Proceedings of the Institute of Mechanical Engineers, Vol. 182, 1967-68, pp. 292-299.

13. D. Dowson and G. R. Higginson, "Elastohydrodynamic Lubrication", Pergamon Press.

14. R. J. Wernick, "Some Computer Results in the Direct Iteration Solution of the Elastohydrodynamic Equations", MTI Report G2TR38, February 1963.

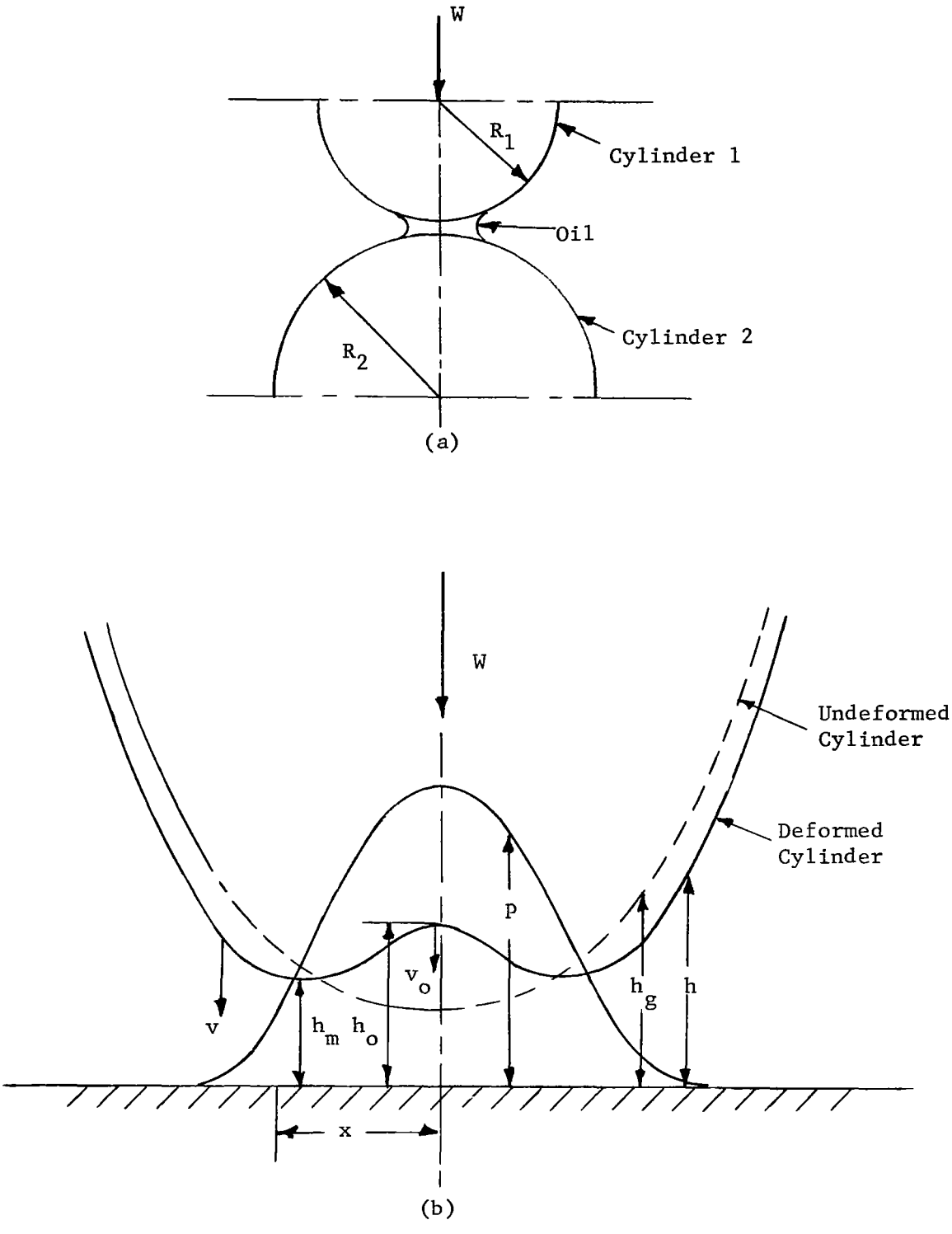

Fig. 1-1 Geometry of the normal approach elastohydrodynamic problem.

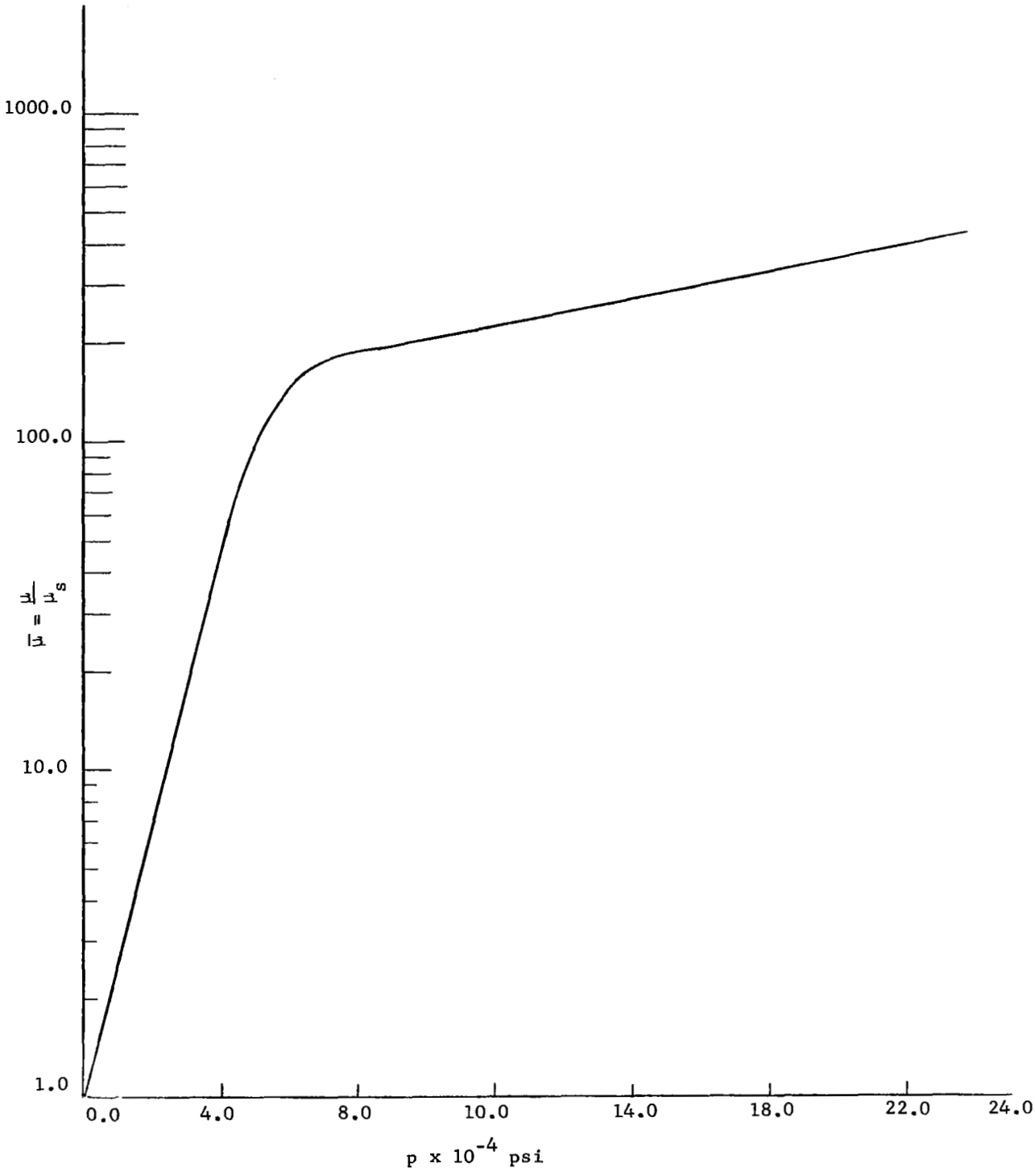

Fig. 1-2 The relation between viscosity and pressure for a composite-exponential lubricant.

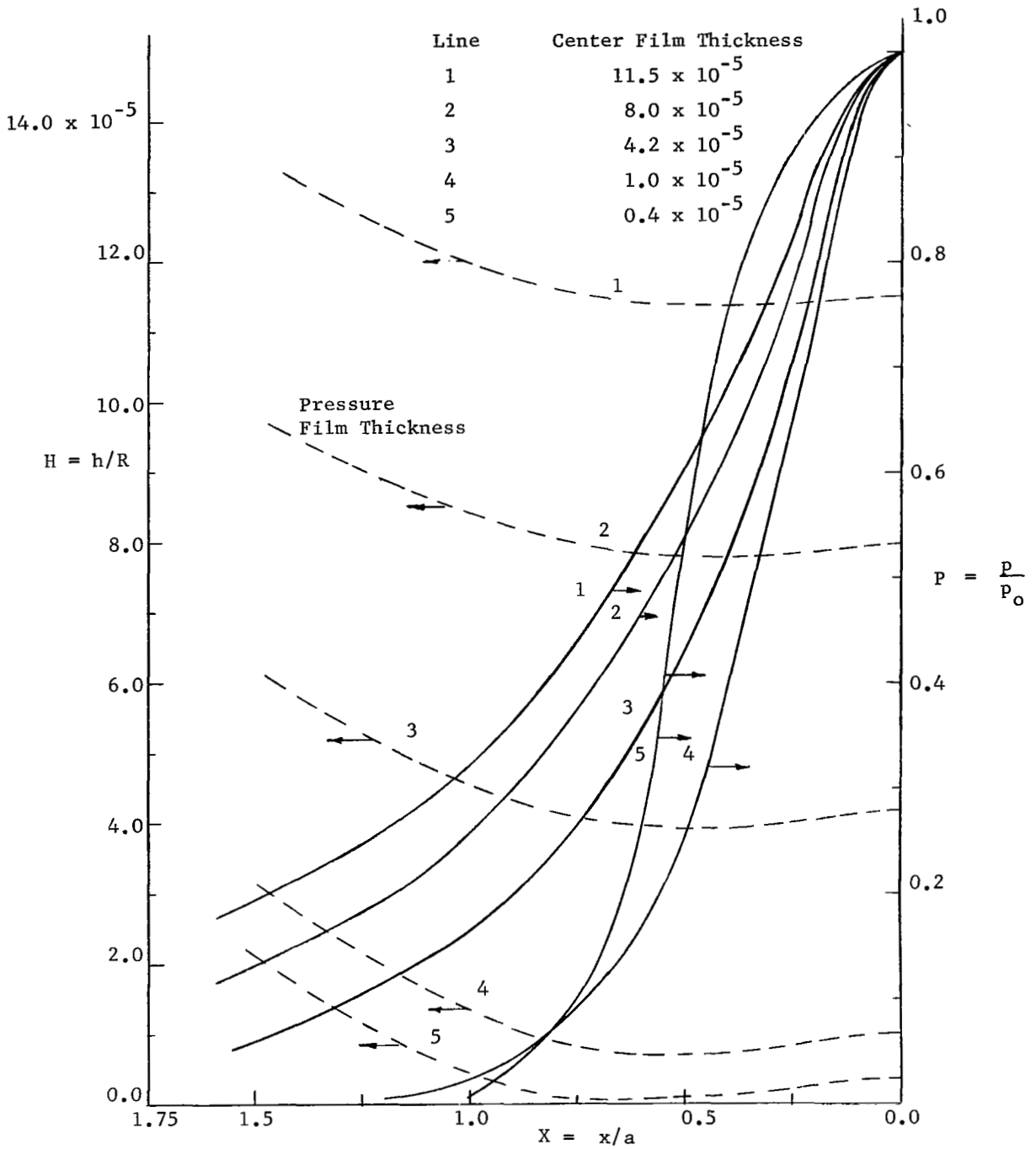

Fig. 1-3 Pressure and deformation profiles, straight exponential lubricant, G = 3180, p_o = 5 x 10^4 psi

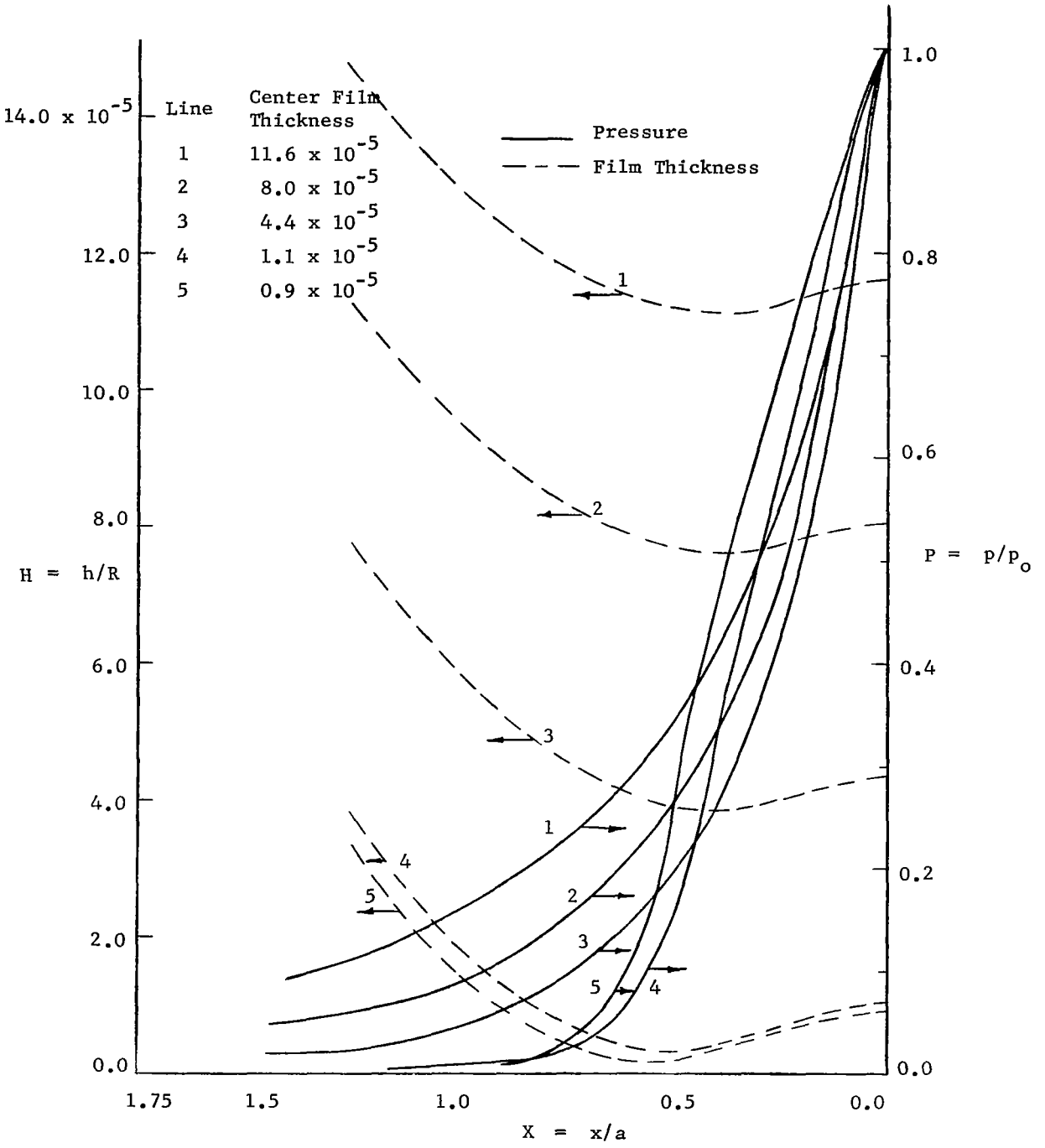

Fig. 1-4 Pressure and deformation profiles, straight exponential lubricant, G = 3180, P_o = 7.5 x 10^4 psi

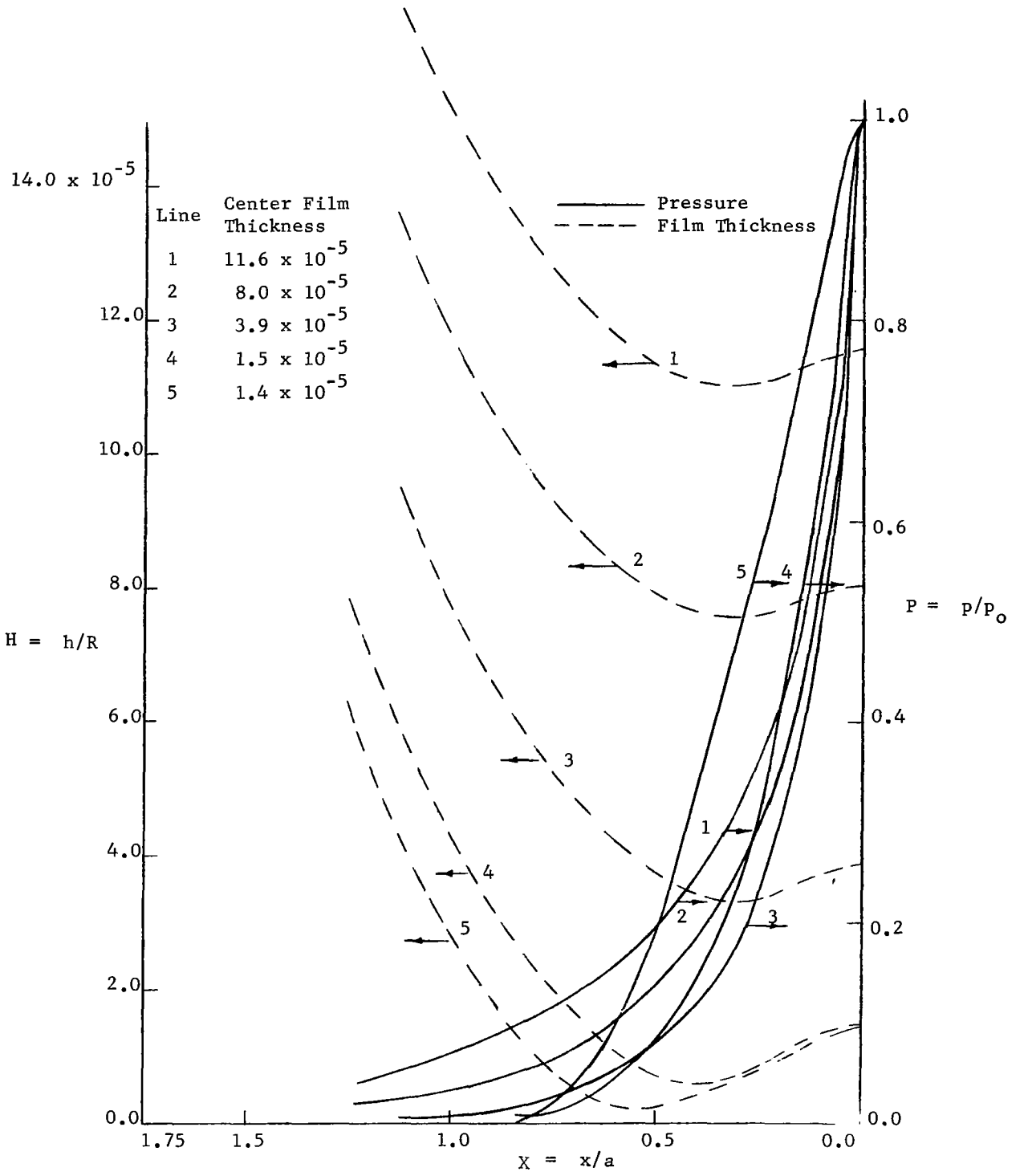

Fig. 1-5 Pressure and deformation profiles, straight exponential lubricant, G = 3180, $p_o = 10^5$ psi

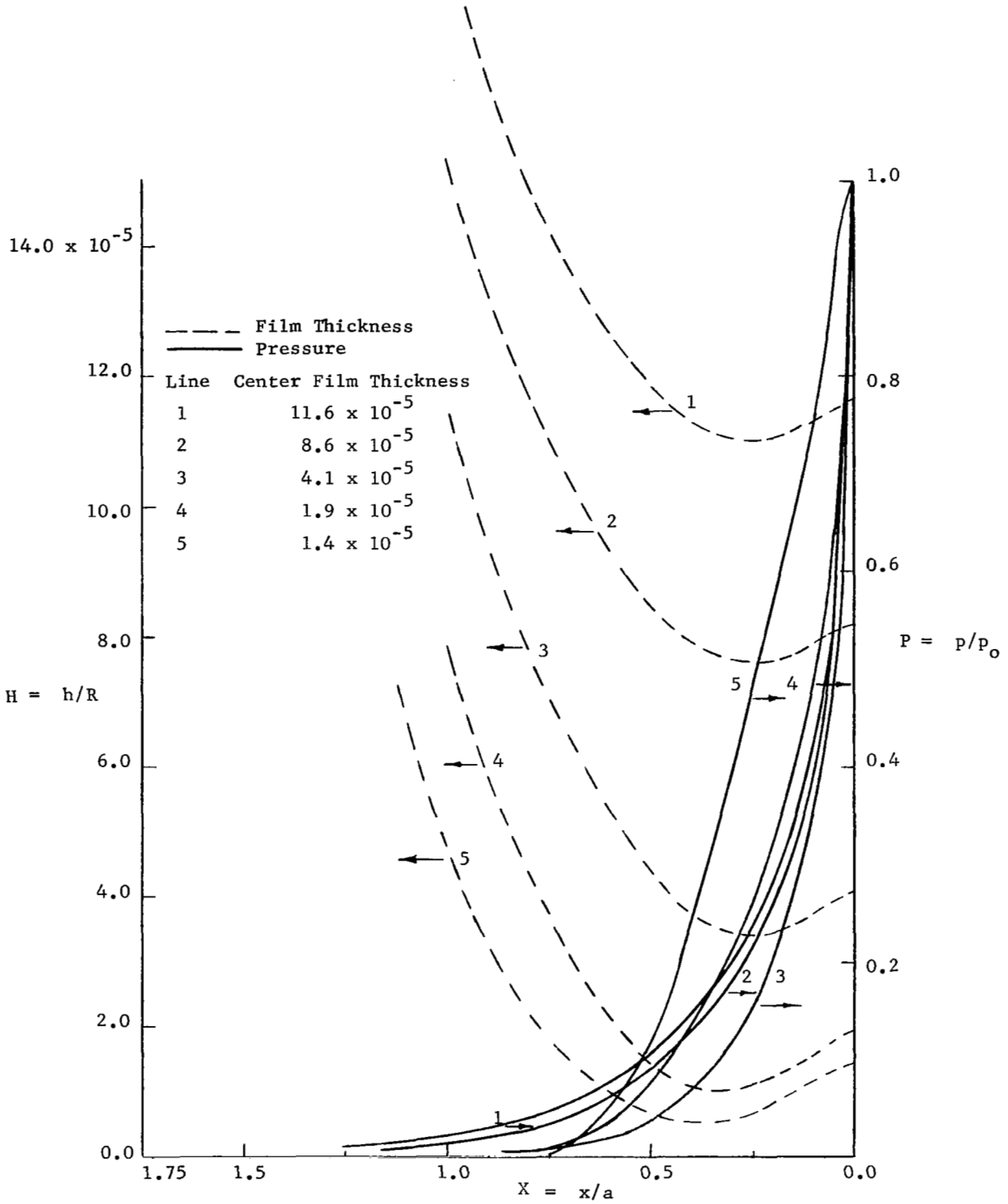

Fig. 1-6 Pressure and deformation profiles, straight exponential lubricant, G = 3180, p_o = 1.25 x 10^5 psi.

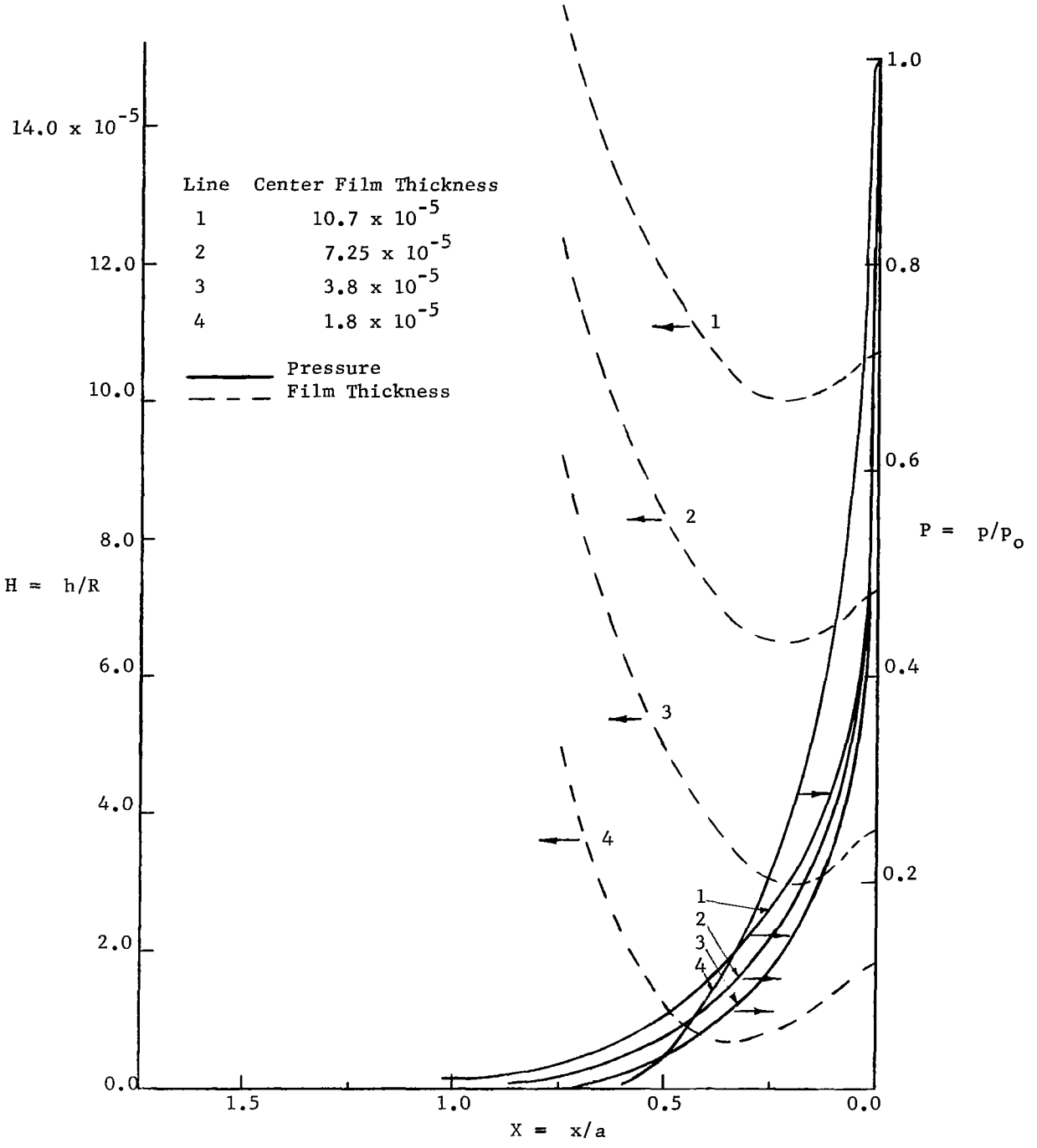

Fig. 1-7 Pressure and deformation profiles, straight exponential lubricant, G = 3180, $p_o = 1.5 \times 10^5$ psi.

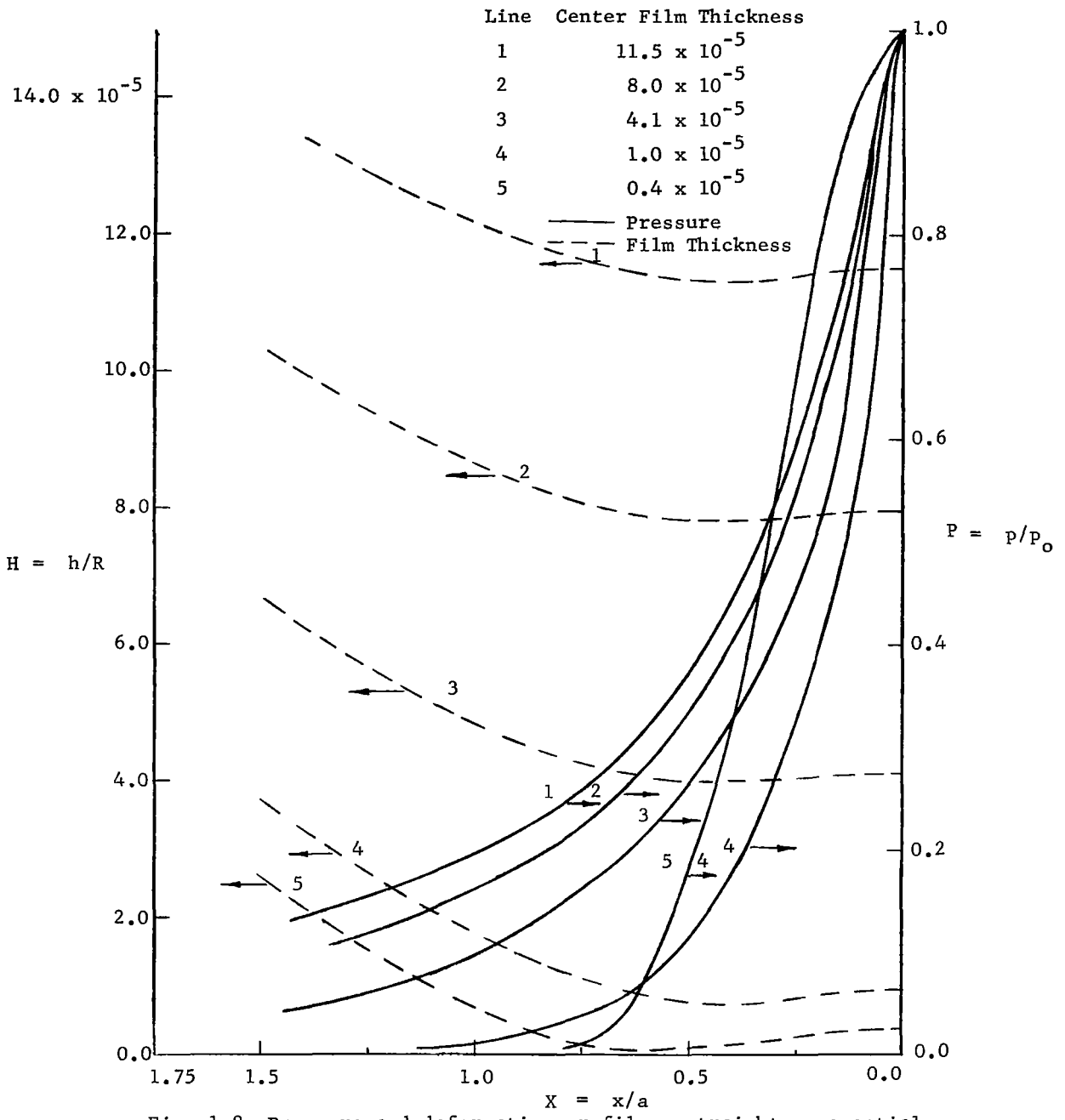

Fig. 1-8 Pressure and deformation profiles, straight exponential lubricant, G = 5000, $p_o = 5.0 \times 10^4$ psi.

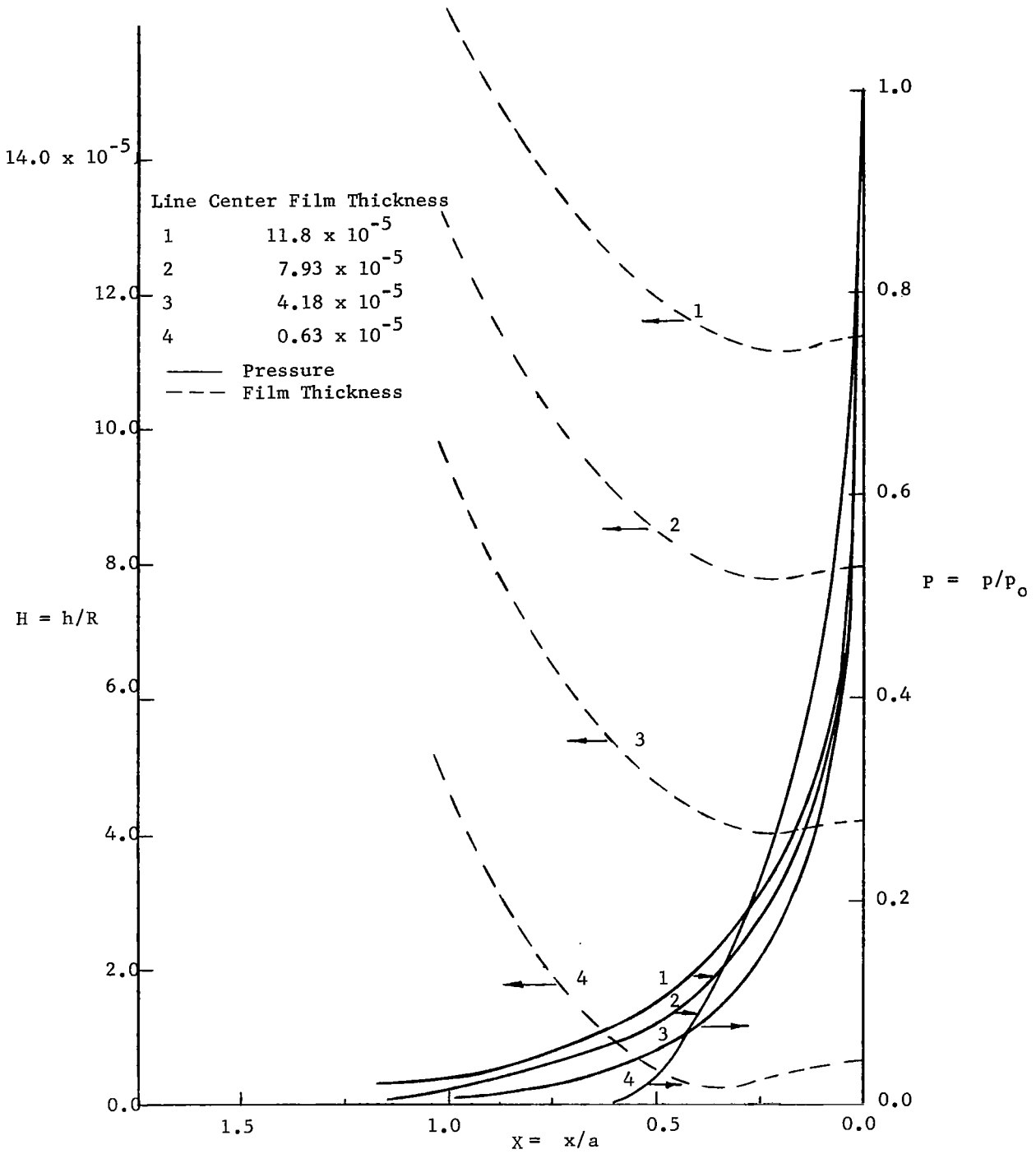

Fig. 1-9 Pressure and deformation profiles, straight exponential lubricant, G = 5000, $p_o = 10^5$ psi.

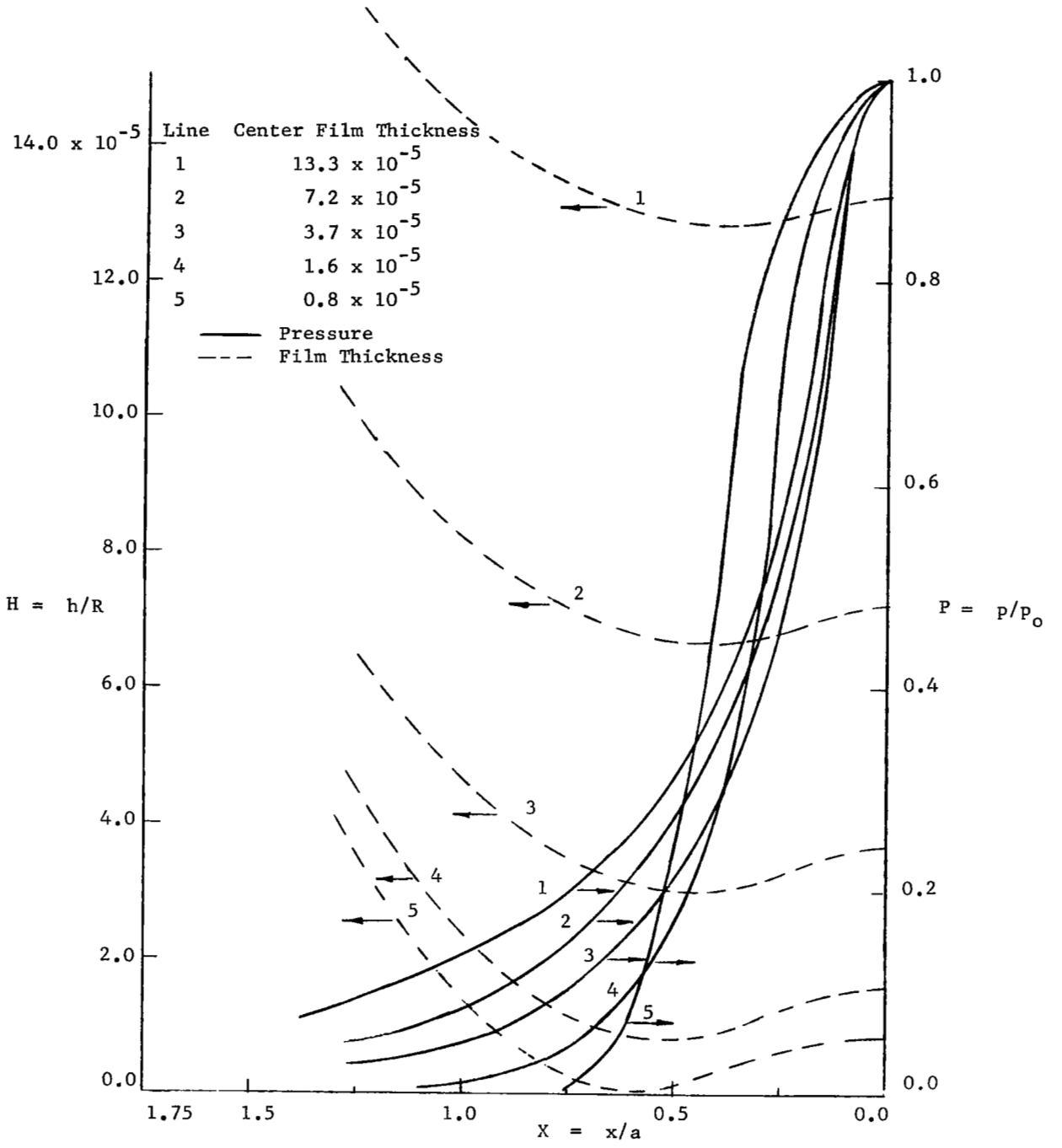

Fig. 1-10 Pressure and deformation profiles, composite exponential lubricant, p_o = 7.5 x 10^4 psi, G = 3180.

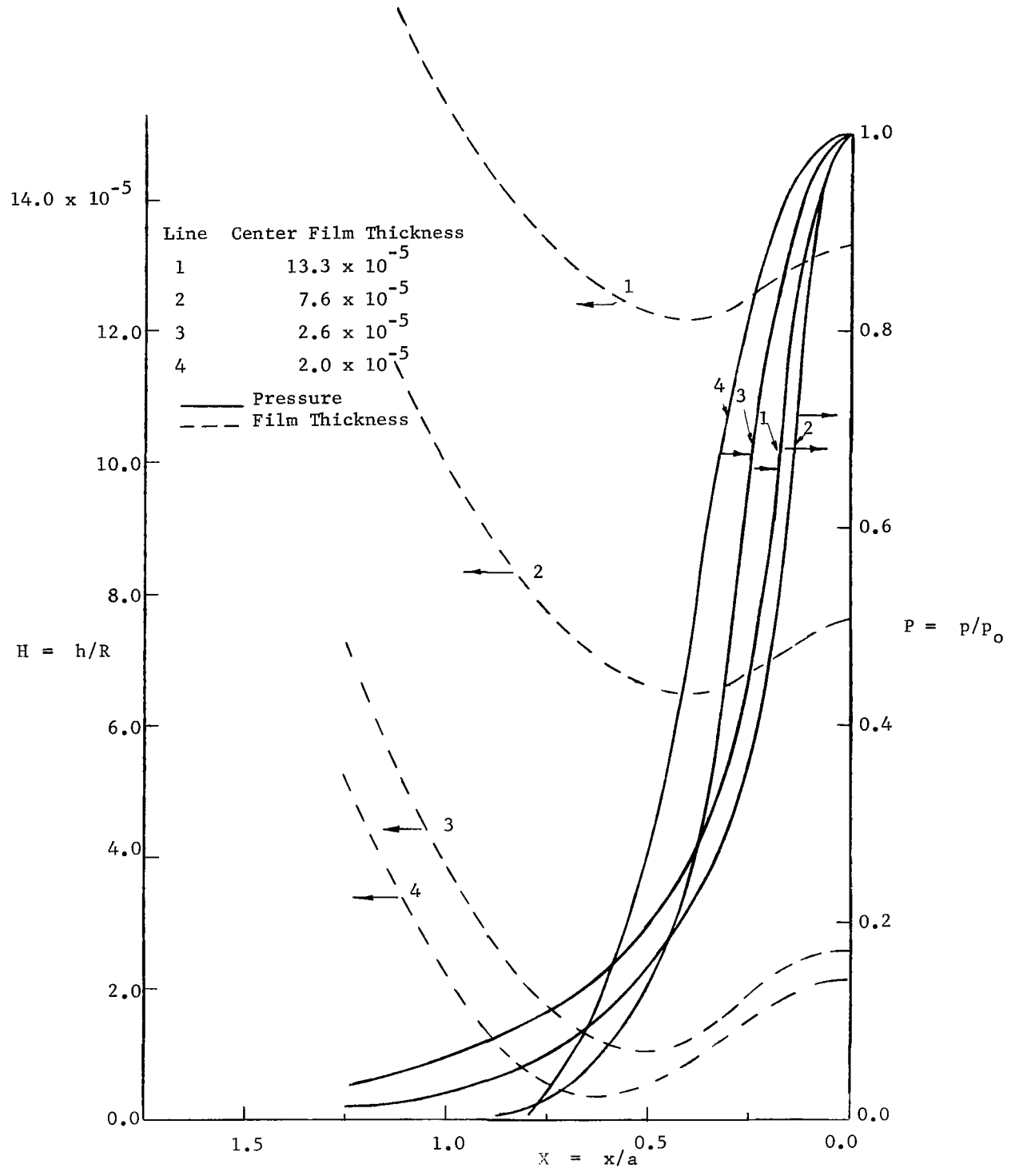

(a) Composite exponential lubricant.

Fig. 1-11 Pressure and deformation profiles, $p_o = 10^5$ psi, G = 3180.

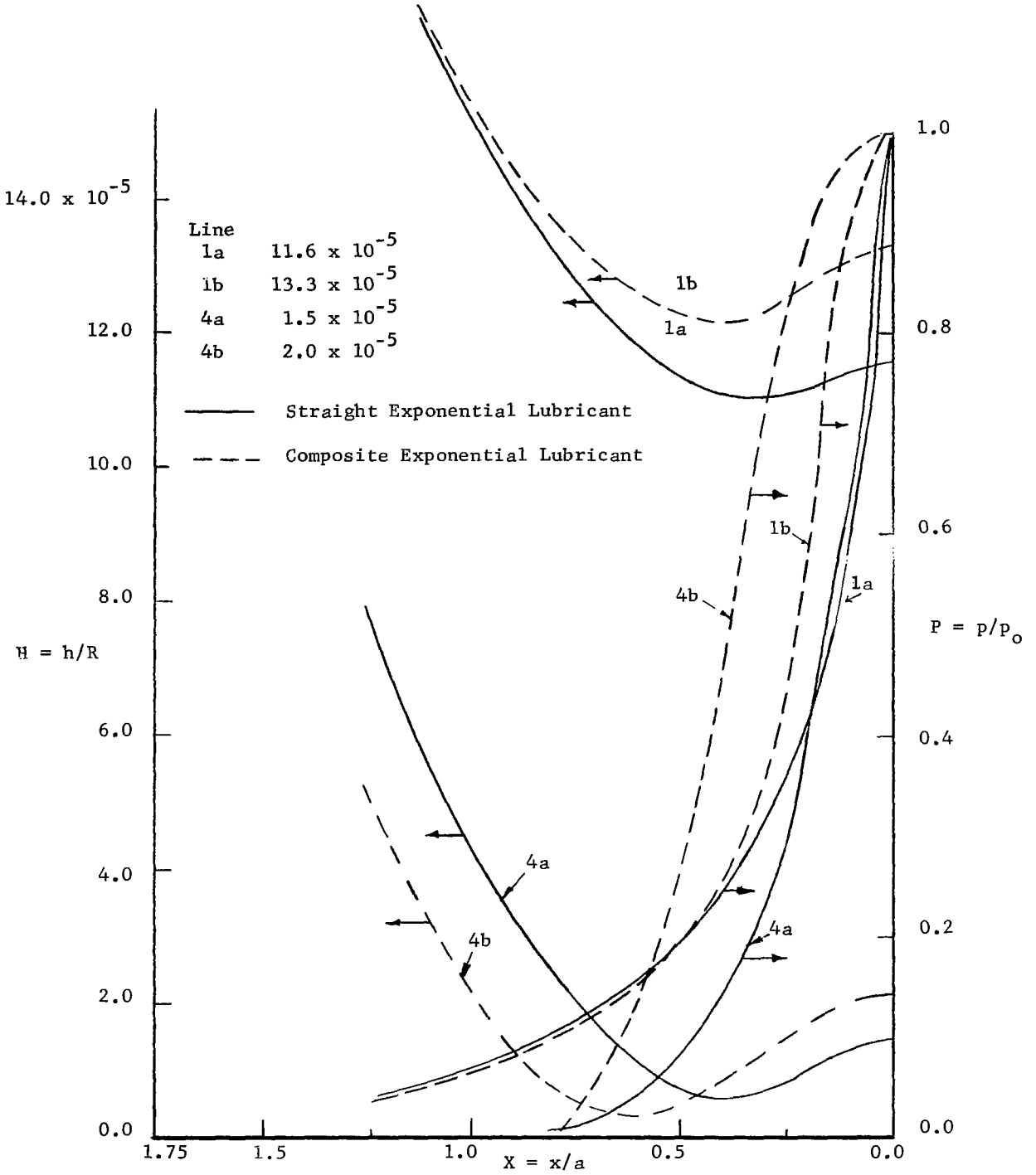

(b) Comparison between straight and composite exponential lubricant.

Fig. 1-11 Pressure and deformation profiles, $p_o = 10^5$ psi, G = 3180.

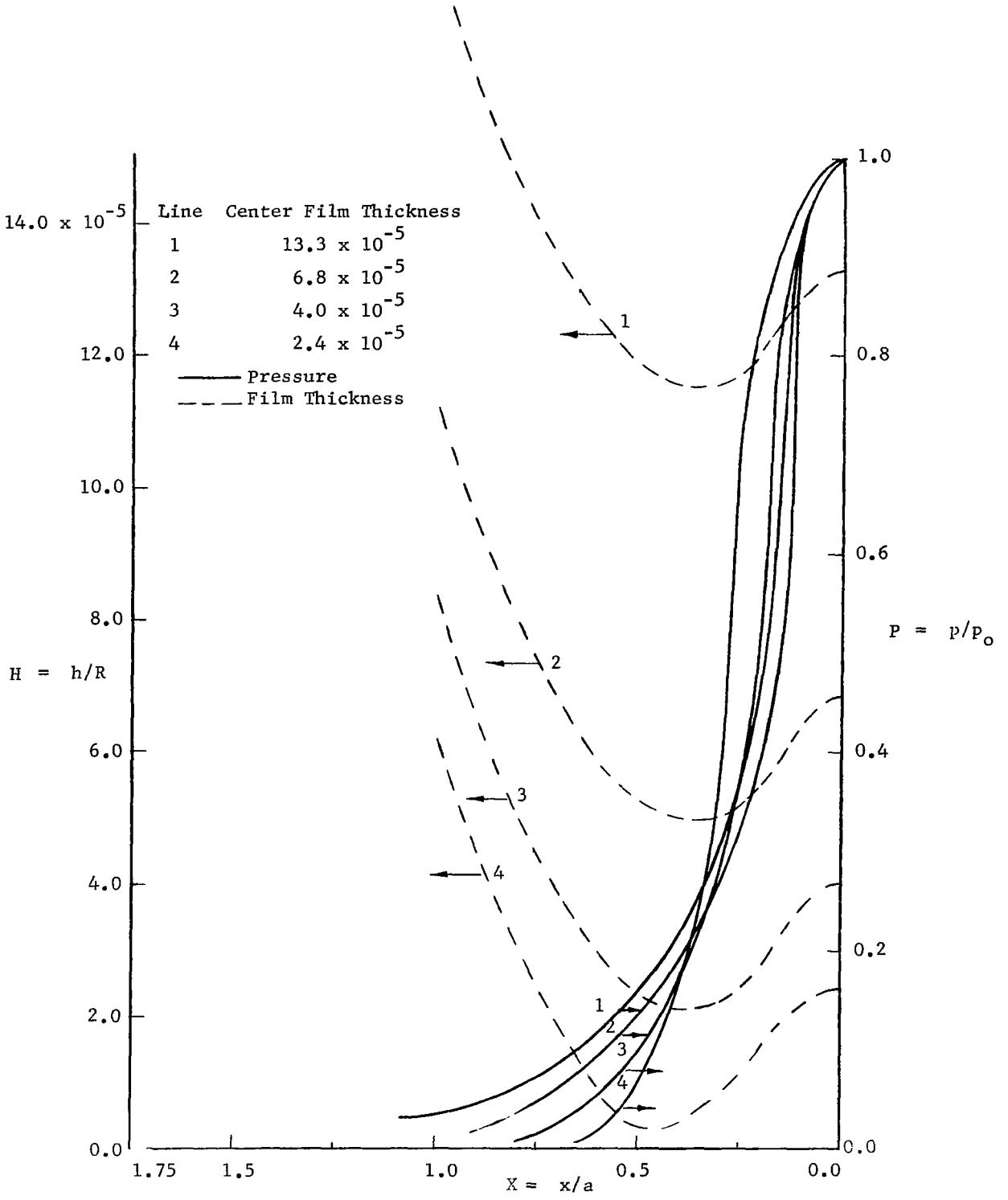

Fig. 1-12 Pressure and deformation profiles, composite exponential lubricant, $p_o = 1.25 \times 10^5$ psi, G = 3180.

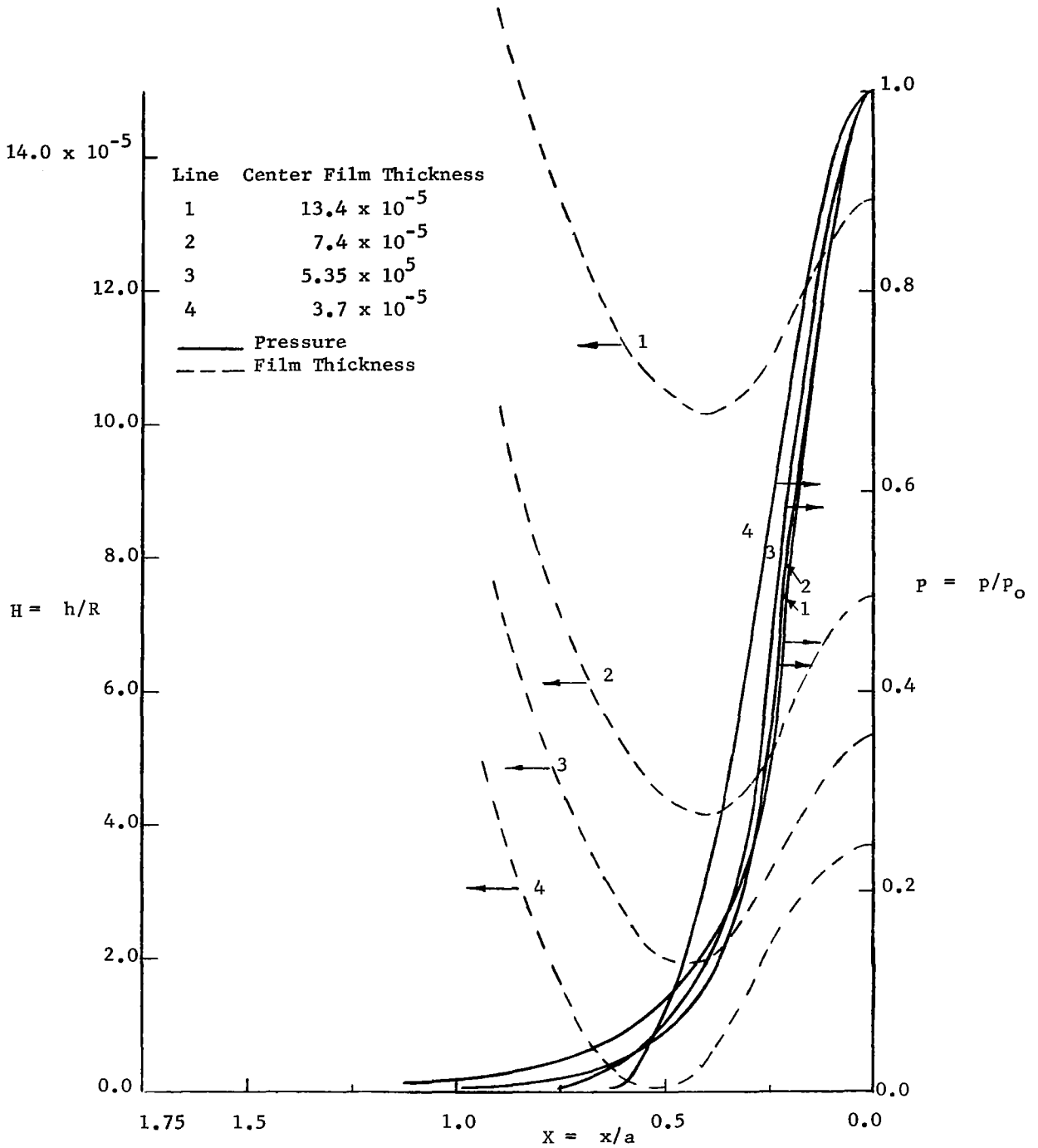

Fig. 1-13 Pressure and deformation profiles, composite exponential lubricant, p_o = 1.5 x 10^5 psi, G = 3180.

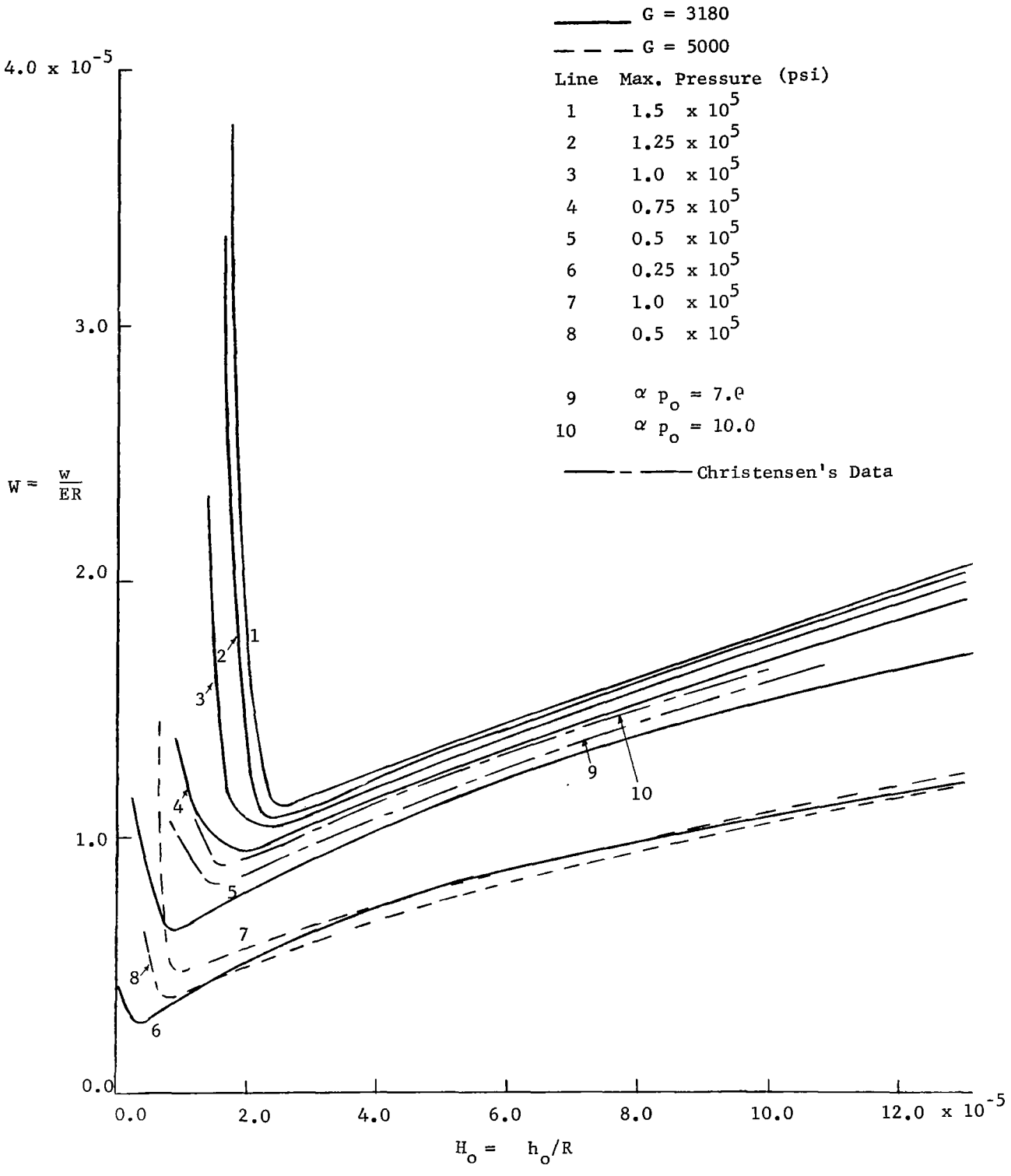

Fig. 1-14 Variation of load with center film thickness, straight exponential lubricant.

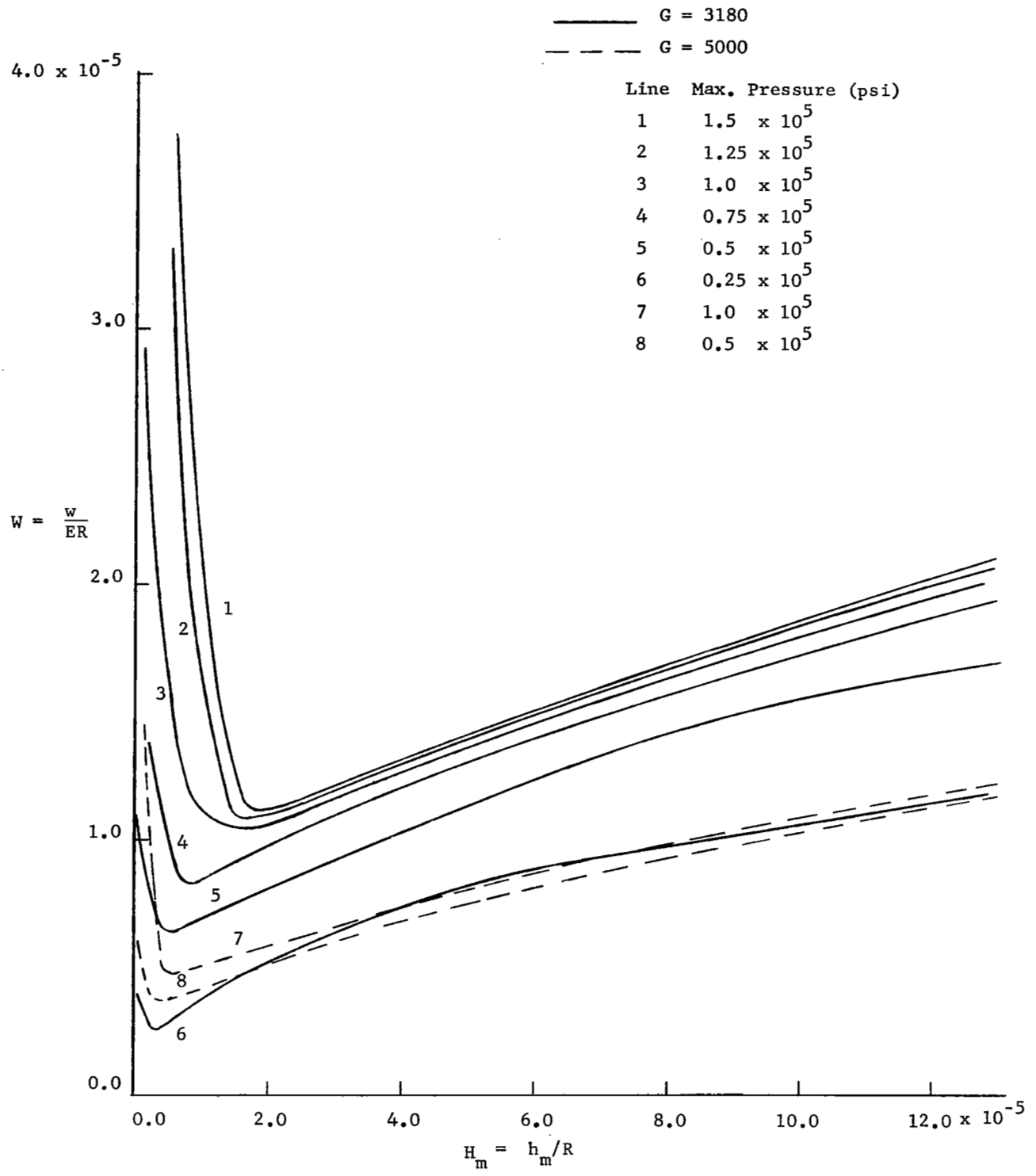

Fig. 1-15 Variation of load with the minimum film thickness, straight exponential lubricant.

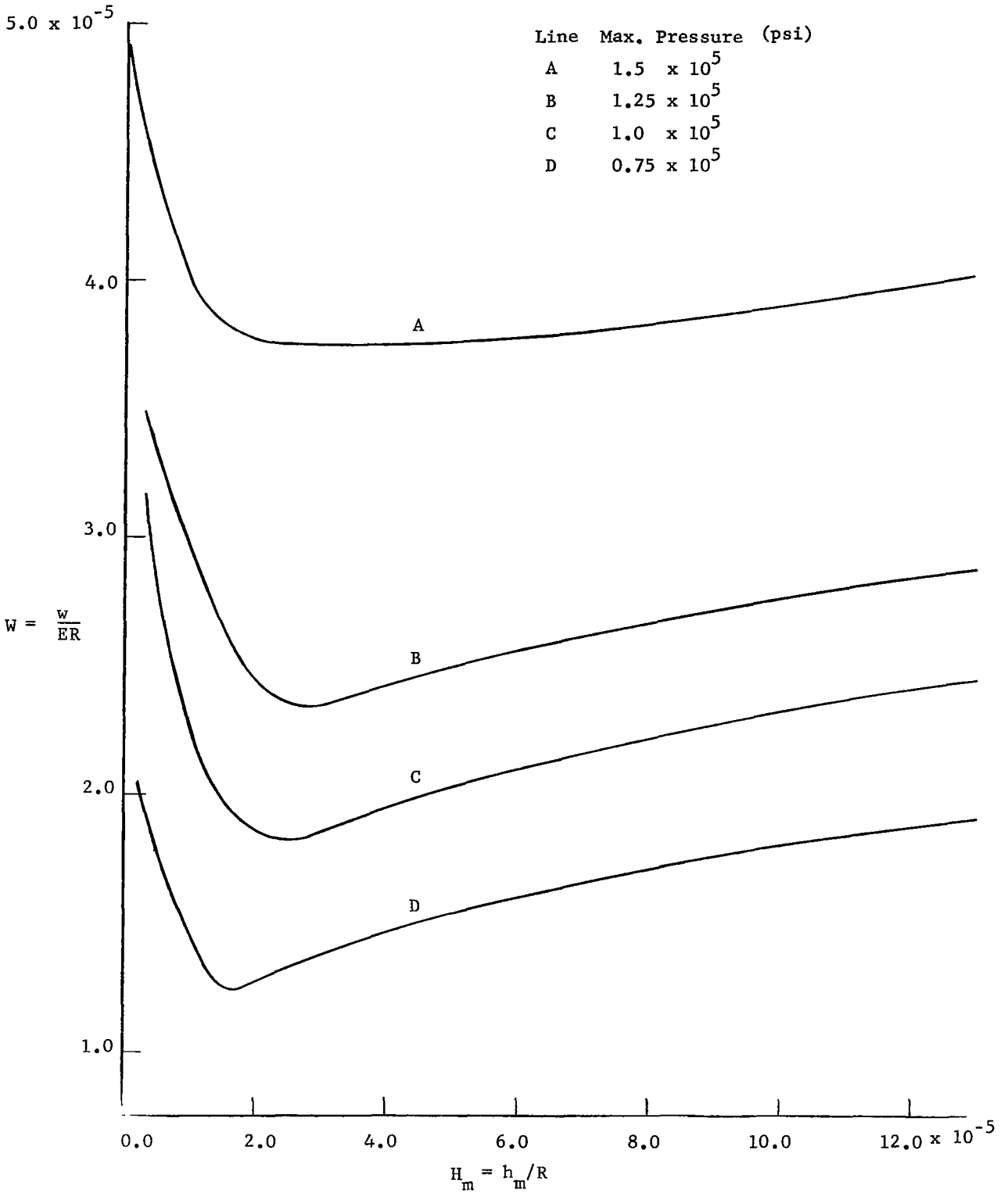

Fig. 1-16 Variation of load with minimum film, composite exponential lubricant.

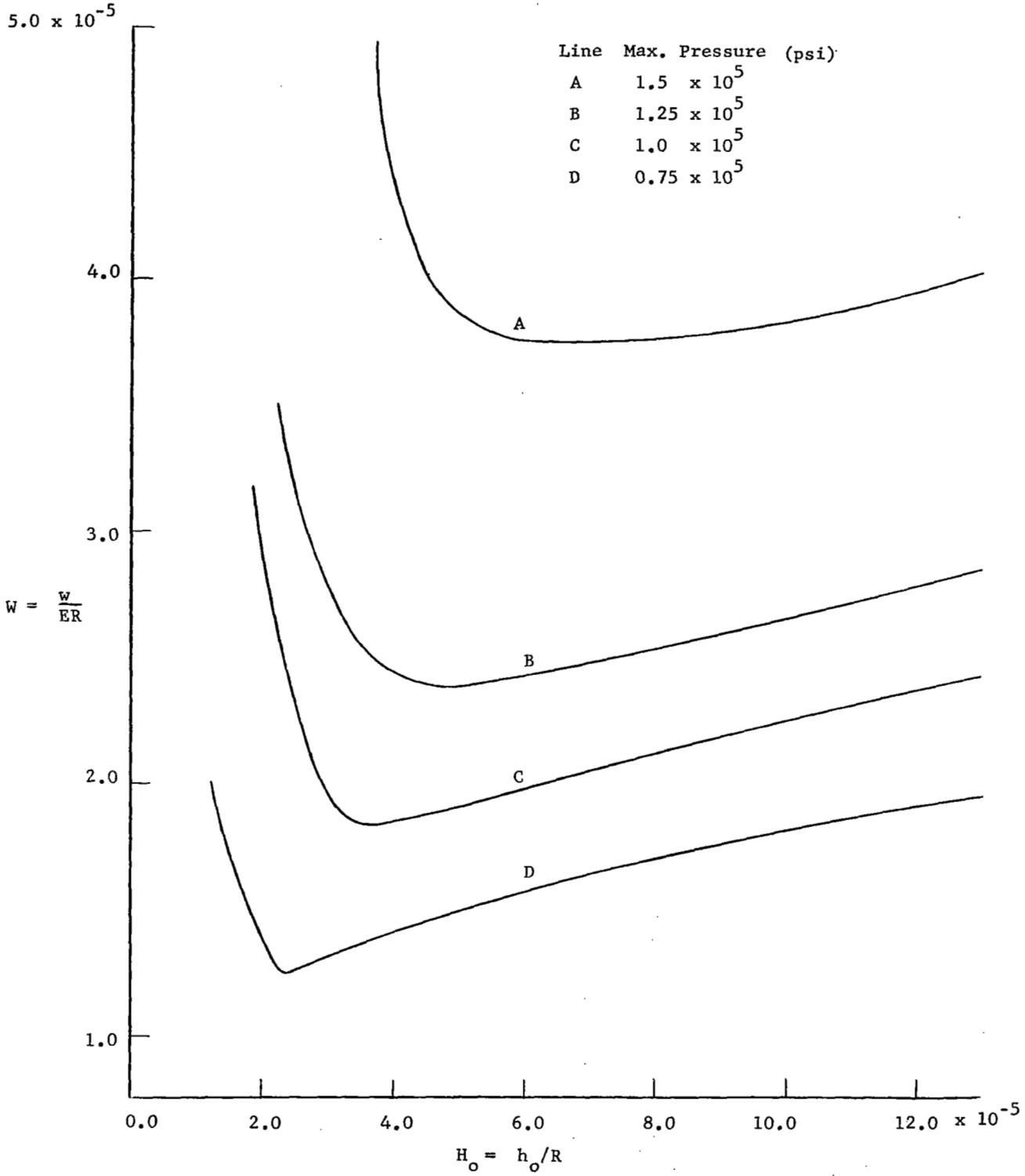

Fig. 1-17 Variation of load with center film, composite exponential lubricant.

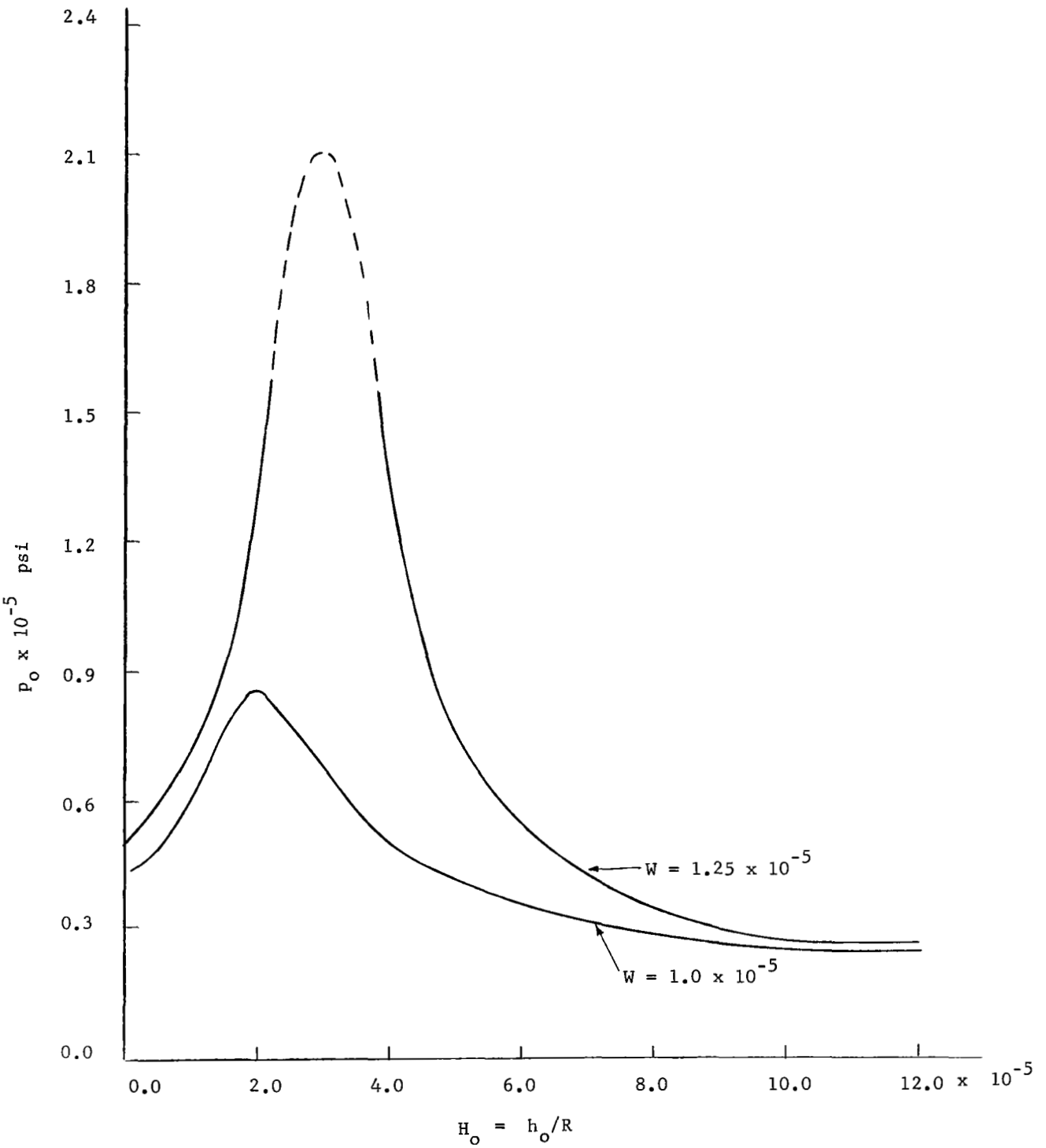

Fig. 1-18 Variation of center pressure with center film for a constant load, straight exponential lubricant.

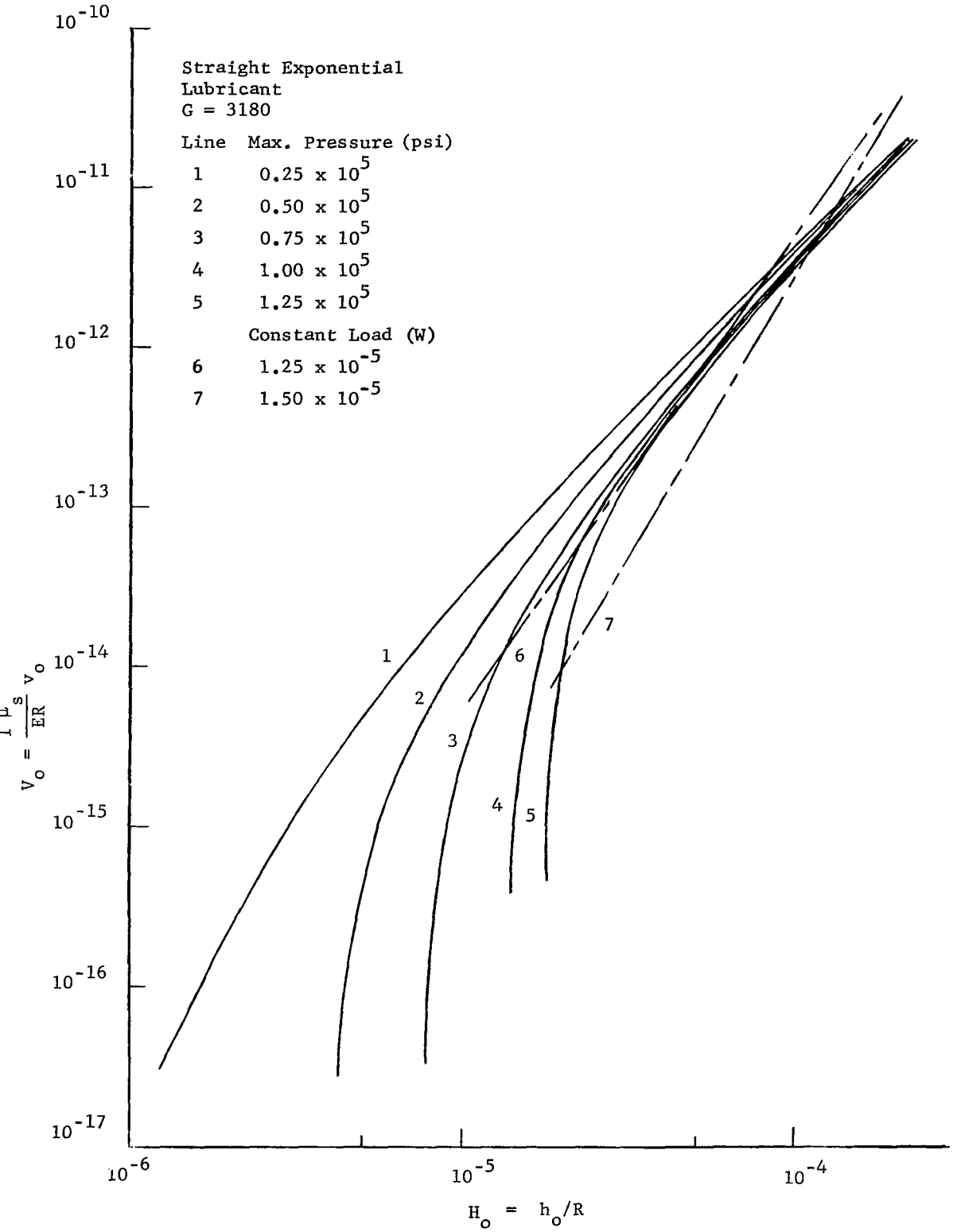

Fig. 1-19 Variation of center approach velocity with center film.

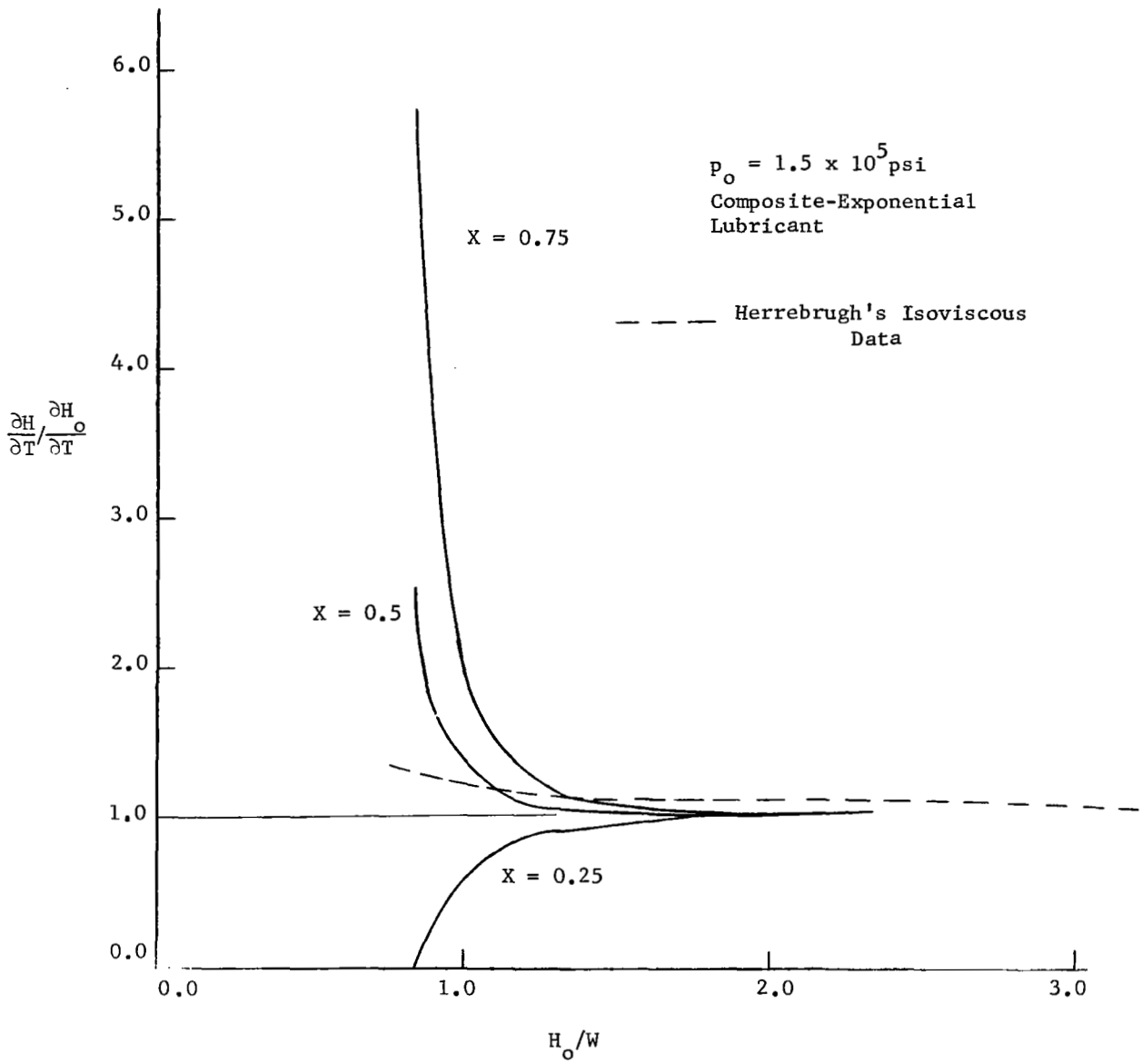

Fig. 1-20 Variation of local approach velocity with the ratio of center film to load.

NASA-Langley, 1971 —— 15 E-6534